10.1071/WF23104
International Journal of Wildland Fire

Supplementary Material

A national accounting framework for fire and carbon dynamics in Australian savannas

Keryn I. Paul[A,*] and *Stephen H. Roxburgh*[A]

[A]CSIRO Environment, GPO Box 1700, ACT 2601, Australia

*Correspondence to: Email: keryn.paul@csiro.au

Supplementary Material

Paul KI and Roxburgh SH (2024) A national accounting framework for fire and carbon dynamics in Australian savannas. International Journal of Wildland Fire 33, WF23104. doi:10.1071/WF23104.

Table of contents

SM-A: Additional information

Pools of biomass

Live woody vegetation

It is assumed that savannas are in a relative steady-state with respect to live woody biomass, with any death of these components (e.g., due to regular mortality and/or stochastic disturbance events) resulting in the recovery of that biomass back to the assumed steady-state. Hence, when simulating a fire event, a small proportion of the live above-ground woody biomass (AGB) of a stand is impacted, or combusted, by the fire (which are assumed to predominantly be smaller trees or shrubs). Of this combusted portion of AGB, some is simulated to be emitted as CO_2-C, while the remainder is simulated to be transferred to dead pools of woody biomass.

Heavy fuel

In addition to live biomass, the savanna vegetation has a significant component (up to 27%) of stags (dead trees or shrubs) (Cook *et al.* 2020; Whitehead *et al.* 2022). As monitored by Whitehead *et al*. (2022), stags slowly senesce and fall to the ground, thereby contributing to coarse woody debris (CWD, 0.6–5 cm diameter). In FullCAM, stags (elevated dead trees or shrubs) and Coarse Woody Debris (CWD, on-ground components of debris ≥ 5 cm diameter) are simulated together as the 'standing dead' pool and defined here as heavy fuel. Inputs of carbon into heavy fuel result from the death of AGB simulated via both regular mortality and stochastic disturbance events such as fire, while losses of carbon from this pool arise from decomposition as well as disturbances such as fire. Given stags and CWD are simulated together as 'standing dead', there is no requirement to predict the time at which stags fall to the ground to become CWD. Although rates of decomposition may differ between stags and CWD (Whitehead *et al.* 2022), an average rate of decomposition is assumed.

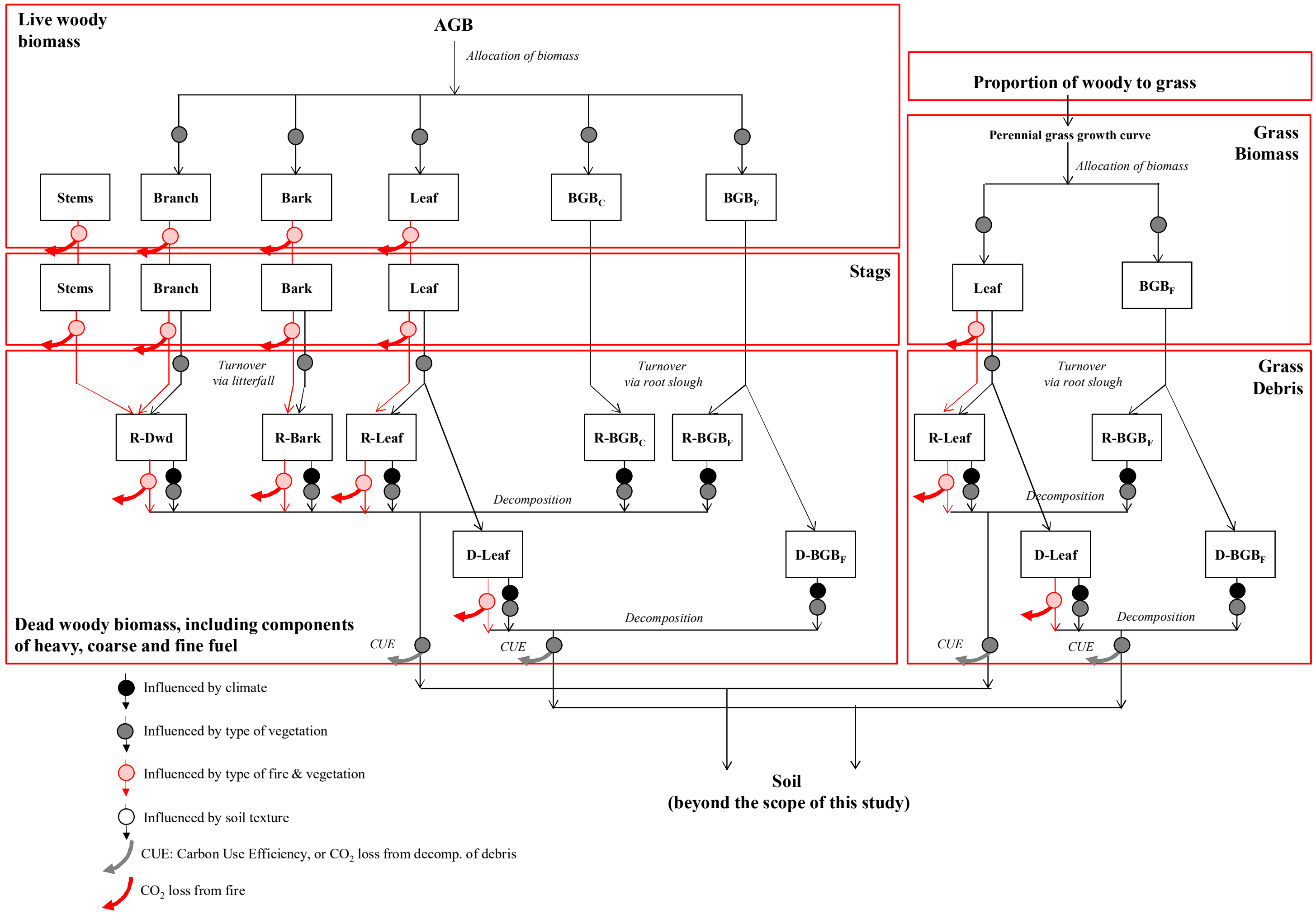

Fig. S1. FullCAM simulated carbon dynamics post-fire. Abbreviations: AGB=Above Ground Biomass, BGB=Below Ground Biomass (with subscripts C and F referring to coarse and fine roots, respectively), Dwd=Dead wood, and R- and D- referring to resistant and decomposable debris, respectively.

Coarse and fine fuel

Predictions of foliage litter were assumed to be fine fuel, while predictions of debris in the form of deadwood and bark litter were assumed to be largely (60%) coarse fuel, with the remainder (40%, e.g., twigs) also contributing to the pool of fine fuel. Inputs of carbon into these pools are simulated through regular turnover of live biomass via litterfall as well as decomposition from the heavy fuel, while losses of carbon are simulated via decomposition (lost carbon being transferred partly to CO_2-C and partly to the soil pools) as well as stochastic disturbance events such as fire (lost carbon being transferred to CO_2-C due to combustion).

Grass fuel

Grass fuel is simulated to include live and dead (grass litter) pools of above-ground biomass. Grass production and die-back is simulated to be seasonal (CoA 2021), with regular inputs to debris via turnover. Within a simulated stand, predicted productivity of live biomass of grass relates to the assumed woody canopy cover of the stand being simulated, e.g., highest in shrublands where woody canopy cover is low, and lowest in forests where woody canopy cover is high. When fire events are simulated, it is assumed a large proportion of both live and dead grass fuel pools are combusted. Although most of this combusted carbon is simulated to be emitted as CO_2-C, a proportion of the combusted carbon in the live grass biomass pool may be simulated to die and thereby transfer to grass litter.

Categories of vegetation

Different savanna vegetation types (Thackway *et al.* 2014; Lynch *et al.* 2018) were found to have differing typical rates of litterfall, decomposition and fire histories, and thus, were previously assumed to have differing fuel accumulation curves (Meyer *et al.* 2015). FullCAM has spatial input layers for fire history, climate and the maximum AGB of woody vegetation (or *M*-layer, Roxburgh *et al.* 2019). Therefore, these spatial input layers, rather than the vegetation category *per se*, were the main drivers of spatial variation in predicted litterfall, decomposition and fuel accumulation. Indeed, the *M*-layer accounted for 75% of the variation in observed AGB of mature stands of savanna (Fig. S2). Nevertheless, it remained important to undertake FullCAM calibrations of shrublands separately from woodlands or open forests given, relative to trees, shrubs are impacted to a greater extent by fires due to their lower heights (Williams *et al.* 1999; Lawes *et al.* 2011; Bond *et al.* 2012). High and low rainfall zones (averages >1,000 mm yr^{-1} and 600-1,000 mm yr^{-1}, respectively) were also considered separately given they differed in terms of their sparseness of woody vegetation, and thus, the extent of grass coverage - the category of fuel most likely to be substantially impacted by fires. This is why the five broad categories of woody vegetation outlined in Table 1 were calibrated.

Additional Tables and Figures

Table S1. Default values applied for estimating the CO_2-e equivalent of methane (CH_4) and nitrous oxide (N_2O) gas emissions due to combustion of live and dead biomass in response to fire in Australian savannas, including the global warming potential, elemental to molecular mass conversion factor, the N:C ratio and the emission factors assumed for these gases during combustion of different fuels under different vegetation types. Data sources: Meyer and Cook (2015); Meyer *et al.* (2015).

Default	Fuel type	CH_4	N_2O
Global Warming Potential (GWP), based on 100 years		25.0	298
Elemental to molecular mass conversion factor		1.333330	1.571429
	Emission factor (E_F) (and N:C ratio)		
WH	Biomass	0.0031	0.0075 (0.0093)
	Heavy fuel	0.0100	0.0036 (0.0081)
	Coarse fuel	0.0031	0.0075 (0.0081)
	Fine or grass fuel	0.0031	0.0075 (0.0096)
WL	Biomass	0.0015*	0.0075 (0.0039)
	Heavy fuel	0.0146*	0.0146 (0.0150)
	Coarse fuel	0.0015*	0.0075* (0.0039)
	Fine or grass fuel	0.0015*	0.0075* (0.0110*)
SH	Biomass	0.0015	0.0066 (0.0093)
	Heavy fuel	0.0100	0.0036 (0.0081)
	Coarse fuel	0.0015	0.0066 (0.0081)
	Fine or grass fuel	0.0015	0.0066 (0.0096)
SL or PL	Biomass	0.0013	0.0059 (0.0039)
	Heavy fuel	0.0111	0.0146 (0.0150)
	Coarse fuel	0.0013	0.0059 (0.0039)
	Fine or grass fuel	0.0013	0.0059 (0.0107)

*Average value observed for the given vegetation type and fuel load.

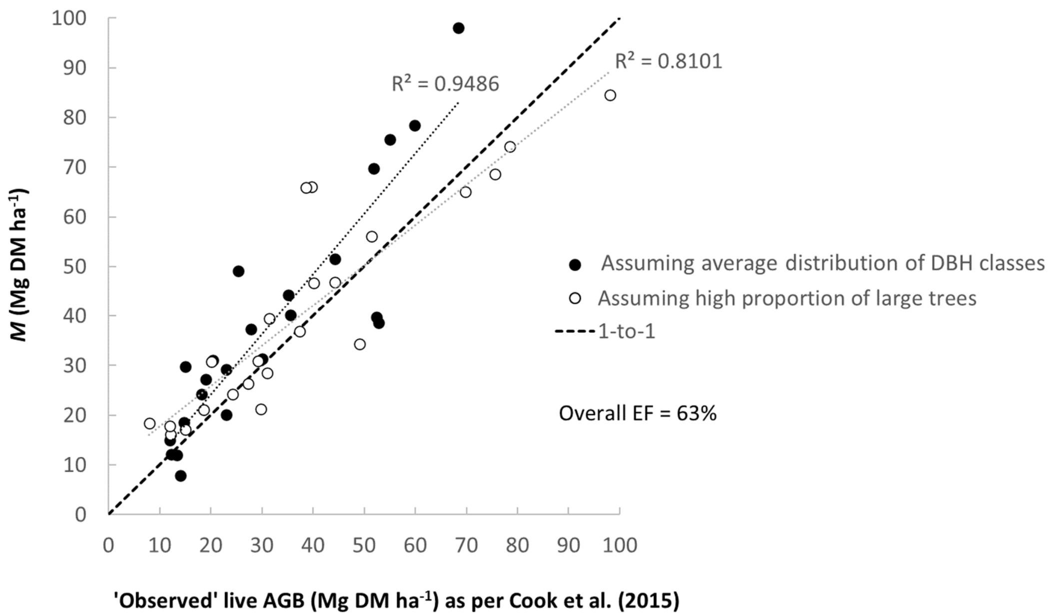

Fig. S2. Relationship between the default *M* (= estimate of the maximum AGB for a given site) as per the FullCAM input layer and the 'observed' live AGB of stands across 23 contrasting biodemographic regions across Australian tropical savannas when the stands were assumed to have a high proportion of large trees. Data source: Cook *et al.* (2015) as reported by Roxburgh *et al.* (2019). Across these regions and assumptions, *M* accounted for 63% of the variation in the 'observed' AGB of mature stands, with *M* typically being, as expected (Supplementary Material B), slightly higher than the average AGB.

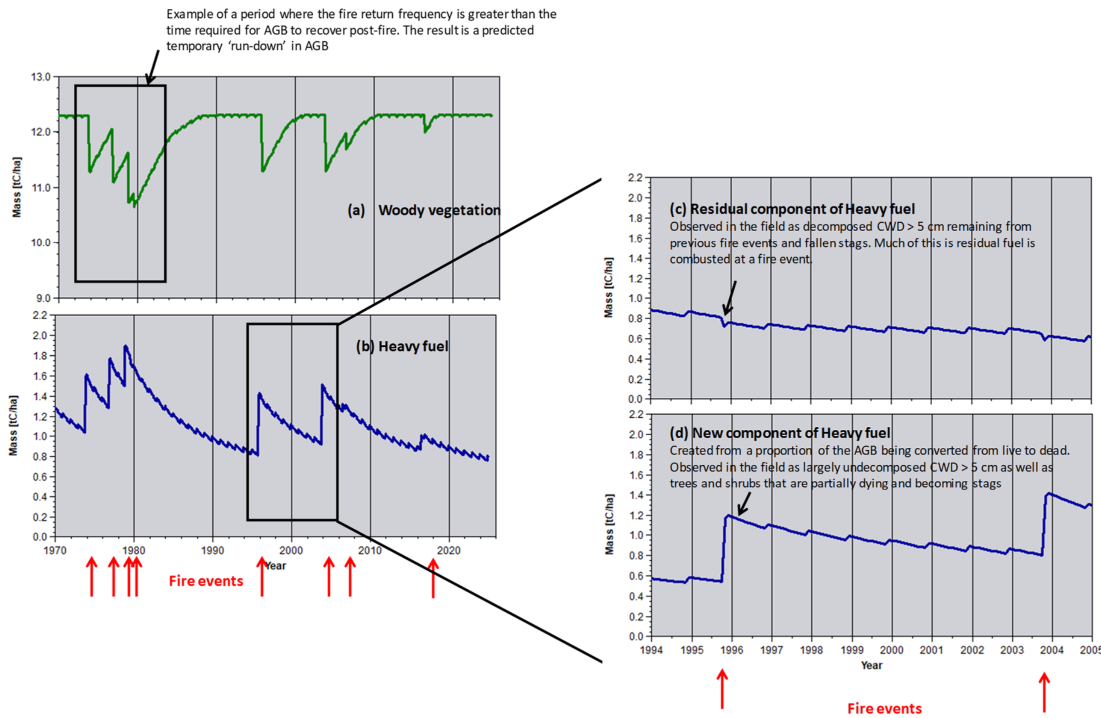

Fig. S3. FullCAM simulation of one example 1 ha plot from the 25 ha PL scenario (SM-D). Outputs include: (a) total biomass carbon in woody vegetation; (b) total biomass carbon in heavy fuel, or what is termed as 'standing dead' in FullCAM; (c) carbon loss from the residual component of heavy fuel in response to a fire event, and; (d) carbon gain from new heavy fuel created in response to a fire event causing some death of live AGB.

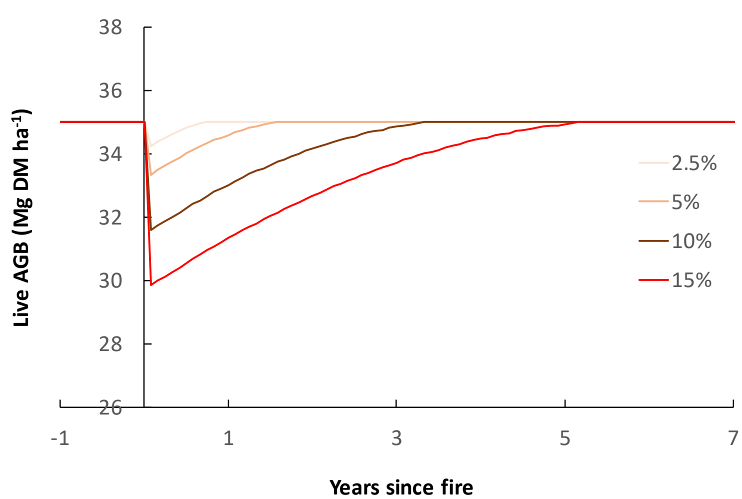

Fig. S4. Theoretical example of how the assumed percentage of fire-impacted AGB (= C_F + T_F) influences FullCAM-predicted recovery times for that pool of AGB. This simulation assumed a pre-fire AGB of 35 Mg DM ha^{-1}. Four scenarios are provided where the AGB is simulated to immediately decreased in response to the fire event by between 2.5% and 15%. Note, due to the paucity of data on fire-impact on specific components of AGB (stem, branches, bark and foliage), the C_F + T_F of a given fire event was assumed to be the same regardless of AGB component.

SM-B: Justification for the assumed impact of fire on dynamics of AGB

For a given effective rainfall (mean annual rainfall less mean annual potential evapotranspiration), the AGB of Australian savannas varies around the average (red line, Fig. S5) due to site-to-site variability in soil nutrients and depth (and thus, water holding capacity) and disturbance histories (fire, drought, wind, grazing). Across these sites, ranges of *M* were higher than those for AGB (blue dashed arrow *cf*. red dashed arrow, Fig. S5) given *M* represents stands that were not recently disturbed (Roxburgh *et al.* 2019). These results were consistent with observations that reducing fire frequencies in Australian savannas leads to an increase in woody biomass and thus greater carbon storage (Grace *et al.*, 2006; Beringer *et al.*, 2007; Murphy *et al.*, 2010; Levick *et al.* 2019). Relationships have been found between the extent of death of live biomass and the frequency and/or intensity of fires (Williams *et al.* 1999; Prior *et al.* 2009; Liedloff and Cook 2007, 2011; Cook *et al.* 2015; Murphy *et al.* 2023). For example, Williams *et al.* (1999) found that over a five-year period of annual burns in an Australian savanna, tree survival was 72% with EDS burning, but only 30% with LDS burning.

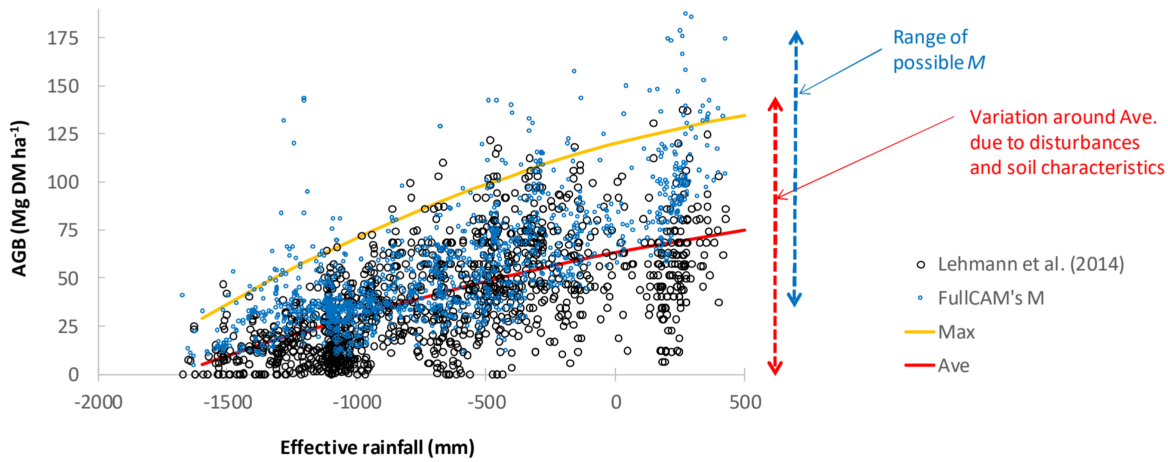

Fig. S5. The observed relationship between AGB in Australian savannas with effective rainfall (= mean annual rainfall minus the mean annual potential evapotranspiration). The data are those assembled by Lehmann *et al.* (2014), but only including sites represented by Australian savanna vegetation types as defined by Thackway *et al.* (2014). Black symbols represent the estimates of AGB via Lehmann *et al.* (2014), while the blue symbols represent the default *M* for that same location. The red line represents a generalised relationship between AGB and effective rainfall, with variation around this average due to variations in the level of past disturbance (fire, recent droughts, wind) and characteristics of the soil (e.g., nutrients and depth and thus, water holding capacity). The blue arrow indicates the range in AGB that corresponds to the range in *M*, which tends to not encompass the relatively low observations of AGB given *M* represent stands that were not recently disturbed yet will vary for any given effective rainfall based on the characteristics of the soil. The yellow line represents the *M* that we might expect for typical sites of a given effective rainfall where soil nutrients and depths are relatively high.

Data from Fig. S5 also provides justification for the assumption that for any given site of a given effective rainfall, the *M* of that site provides an indication of the potential increase of stand AGB from reducing disturbance from fires, and not the upper bound of *M* (yellow line, Fig. S5). Clearly rainfall (rather than fire) is a key driver of AGB in Australian savannas (Lehmann *et al.* 2014; Murphy *et al.* 2015), indicating the importance of competition between trees (or shrubs) for resources such as water. Only a site of optimal soil nutrient and water holding capacity may be represented by the upper bound of *M* for a given effective rainfall (yellow line, Fig. S5). The importance of this inter-tree competition explains why there was only a 3.5% increase in basal area in a five-year fire exclusion study (Williams *et al.* 1999; Andersen *et al.* 2003), while after nine-years of fire exclusion AGB did not significantly differ from adjacent plots which were regularly burnt (Levick *et al.* 2019). It also explains why following removal of competition from overstorey trees, dense regrowth of saplings emerges despite frequent fires in Australian savannas (e.g., Wilson and Bowman 1987; Fensham and Bowman 1992; Cook and Goyens 2008; Freeman *et al.* 2017).

Based on the assumption that inter-tree competition for resources is the main factor limiting AGB in Australian savannas, it was assumed M is not changed by a management-imposed reduction in fire intensity. Nevertheless, EDS prescribed burning will ensure that the stand has AGB closer to M for a greater proportion of time, thereby potentially increasing AGB when averaged over a period. The extent of predicted increase in carbon stored in AGB in response to a fire management project will therefore be influenced by the combination of: (i) sensitivity to fire, and thus, vegetation type, (ii) extent of fire-induced suppression of AGB below M, which in turn will depend on the fire frequencies and severities during the pre-project baseline period, and (iii) changes in fire frequency and intensity.

Given the importance of M in providing the upper limit for AGB increases following savanna fire management, an accurate estimate of this input was required for each calibration site. Although M (calibrated based on predictor variables of 0-30 cm total soil organic carbon and average climatic conditions, Roxburgh *et al.* (2019)) was well verified for savanna vegetation overall (Fig. S2), for any given stand, M may be inaccurate depending on fine-scale spatial variably associated with position within the landscape of that stand, and hence, soil nutrients and depth (and thus, water holding capacity). Therefore, to ensure the assumed M was as accurate as possible for the calibration stands simulated, field-based measurements of maximum AGB were applied to estimate M in preference to the default M for that stands location. This was achieved by assuming field-based M was: (i) the maximum observed among AGB observations made at varying times for stands that had repeat measurements, (ii) maximum of the observed AGB among a cluster of transects that were measured to represent replicates within 'study site', and (iii) observed AGB. Clearly, (i) stands had estimates of *M* of highest confidence, and therefore, only these stands were used to calibrate the impact of fires on live biomass. For these stands there was a general overall agreement between these alternative estimates of *M* (Fig. S6).

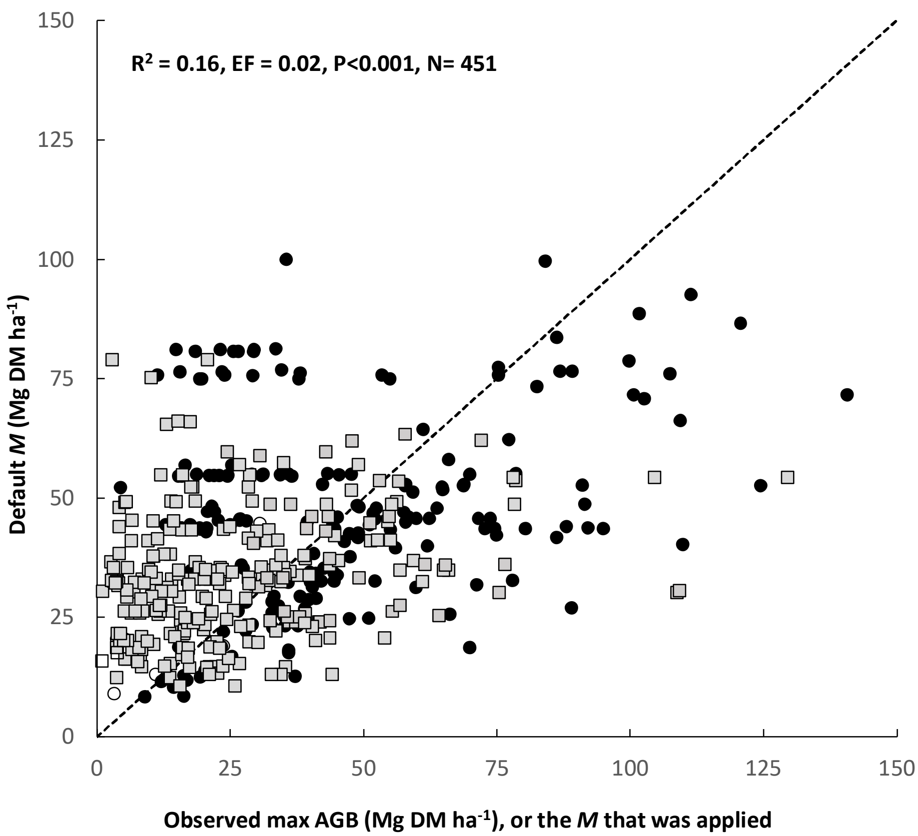

Fig. S6. Relationship between the default *M* and the *M* that was applied for each plot simulation based on the maximum of the AGB observations for each plot over its period of monitoring. Most points in the plots of observed maximum AGB *vs.* predicted *M* were clustered around the 1:1 line, although as expected, the default *M* estimates providing significant under- or over-estimates of maximum AGB for any given stand (Roxburgh *et al.* 2019). Circle symbols represent WH and SH, while square symbols represent WL and SL.

SM-C: Calculating 'observed' AGB and fuel pools

Live biomass

Pools of 'observed' live biomass within calibration stands were estimated using datasets of transect-based inventories that recorded equivalent stem diameter (measured at 10 or 130 cm above the ground: D_{10} or D_{130}, respectively), PFT and heath (live or dead), where PFT is the plant functional types as defined by Paul *et al.* (2016; 2019) and listed in Table S2. Although height rather than D_{10} was often measured for shrubs, shrub height was empirically related to shrub D_{10} (Fig. S7).

Using PFT-based allometric equations verified for savanna systems (Figs. S8 and S9), D_{10} or D_{130} measurements of live individuals were applied to estimate above-ground biomass (AGB; Paul *et al.* 2016) and below-ground biomass (BGB; Paul *et al.* 2019). Plant-level biomass estimates were then scaled-up to the stand-level (Mg DM ha^{-1}) by summing the biomass of all individuals of the various PFTs measured within the area of the transect (Table S3).

Table S2 [Next page]. Species allocated to plant functional types (PFT), as defined by Paul *et al.* (2016; 2019). The PFTs included 'Eucalypt trees' (Euc), 'Other trees' (high or low wood density; Other-H and Other-L, respectively), 'Multi-stemmed acacias' (Multi), and 'Shrubs'.

Euc[1]	Multi[2]	Other-H[3]	Other-H[3] cont.	Other-L[4]	Shrub
Corymbia aparrinja	Acacia argyrodendron	Adansonia gregorii	Melaleuca citrolens	Alstonia actinophylla	Acacia colei
Corymbia arnhemensis	Acacia bidwillii	Alectryon oleifolius	Melaleuca minutifolia	Blepharocarya depauperata	Acacia farnesiana
Corymbia aspera	Acacia coriaceae	Allocasuarina luehmannii	Melaleuca nervosa	Brachychiton australis	Acacia holosericea
Corymbia bella	Acacia cowleana	Alphitonia excelsa	Melaleuca quiquinervia	Brachychiton diversifolius	Acacia lachnophylla
Corymbia bleeseri	Acacia crassicarpa	Alstonia constricta	Melaleuca viridiflora	Brachychiton megaphyllus	Acacia lamprocarpa
Corymbia chartace	Acacia eriopoda	Antidesma ghesaembilla	Owenia acidula	Brachychiton obtusilobus	Acacia monitcola
Corymbia citriodora	Acacia excelsa	Archidendropsis basaltica	Owenia vernicosa	Brachychiton paradoxus	Acacia victoriae
Corymbia clarksoniana	Acacia flavescens	Atalaya hemiglauca	Persoonia falcata	Erythrina vespertilio	Apophyllum anomalum
Corymbia clarksonii	Acacia harpophylla	Banksia dentata	Petalostigma banksii	Gyrocarpus americanus	Breynia oblongifolia
Corymbia collina	Acacia melanoxylon	Bauhinia arborescens	Petalostigma pubescens	Litsea glutinosa	Calytrix achaeta
Corymbia confertiflora	Acacia platycarpa	Bauhinia cunninghamii	Pittosporum phylliraeoides		Calytrix arborescens
Corymbia cullenii	Acacia salicina	Brachychiton populneus	Planchonella arnhemica		Calytrix brownii
Corymbia dampieri	Acacia shirleyi	Brachychiton diversifolius	Planchonia canescens		Calytrix exstipulata
Corymbia dichromophloia	Acacia tumida	Breynia cernua	Planchonia careya		Carissa lanceolata
Corymbia disjuncta		Bridelia tomentosa	Pleiogynium timoriense		Carissa ovata
Corymbia drysdalensis		Buchanania arborescens	Pouteria arnhemica		Citrus gracilis
Corymbia dunlopiana		Buchanania obovata	Pouteria sericea		Cycas sangulata
Corymbia erythrophloia		Bursaria incana	Premna acuminata		Denhamia cunninghamii
Corymbia ferruginea		Bursaria spinosa	Pseudopanax crassifolius		Denhamia oleaster
Corymbia flavescens		Callitris glaucophylla	Quintinia spp.		Dodonaea physocarpa
Corymbia foelscheana		Callitris intratropica	Santalum lanceolatum		Dodonaea viscosa
Corymbia grandifolia		Canarium australianum	Stenocarpus acacioides		Ehretia saligna
Corymbia greeniana		Canthium attenuatum	Strychnos lucida		Eremophila longifolia
Corymbia kombolgiensis		Canthium odoratum	Syzygium eucalyptoides		Eremophila mitchellii
Corymbia latifolia		Canthium oleifolium	Syzygium suborbiculare		Eremophila species
Corymbia leichardtii		Canthium vaciniifolium	Terminalia aridicola		Erythroxylum australe
Corymbia oocarpa		Capparis canescens	Terminalia canescens		Flueggia virosa
Corymbia opaca		Capparis lasiantha	Terminalia carpentariae		Gardenia ewartiana
Corymbia papuana		Capparis mitchellii	Terminalia ferdinandiana		Gardenia ochreata
Corymbia peltata		Capparis spinosa	Terminalia ferdinaniana		Gardenia pyriformis
Corymbia polisciada		Capparis umbonata	Terminalia grandiflora		Gardenia vilhelmii
Corymbia polycarpa		Carallia brachiata	Terminalia latipes		Grevilea refracta
Corymbia polysciada		Cassia brewsteri	Terminalia oblongata		Grevillea decurrens
Corymbia porrecta		Cassia tomentella	Terminalia platyptera		Grevillea glauca
Corymbia ptychocarpa		Clerodendrum floribundum	Terminalia pterocarya		Grevillea heliosperma
Corymbia rhodops		Cochlospermum fraseri	Terminalia volucris		Grevillea parallela
Corymbia setosa		Cochlospermum gillivraei	Vachellia pachyphloia		Grevillea pterosperma
Corymbia terminalis		Coelespermun reticulatum	Vachellia pallidifolia		Grevillea wickhamii
Corymbia tessellaris		Croton arnhemicus	Ventilago viminalis		Hakea chordophyl
Corymbia trachyphloia		Cryptostegia grandiflora	Verticordia cunninghamii		Hakea fraseri
Corymbia zygophylla		Cupaniopsis anacardioides	Vitex glabrata		Jacksonia dilatata
Eucalyptus acmenoides		Denhamia ferdinandii	Wrightia pubescens		Jasminum didymum
Eucalyptus alba		Denhamia obscura	Xanthostemon		Jasminum racemosum
Eucalyptus bella		Diospyros calycantha	eucalyptoides		Lantana camara
Eucalyptus bigalerita		Diospyros humilis	Xanthostemon paradoxus		Lysiphyllum gilvum
Eucalyptus brachyandra		Dolichandrone filiformis	Xanthostemon species		Maytenus cunninghamii
Eucalyptus brevifolia		Dolichandrone heterophylla	Zyziphus mauritiana		Miliusa traceyi
Eucalyptus brownii		Drypetes deplanchei			Myoporum
Eucalyptus cambageana		Ehretia membranifolia			Opuntia tomentosa
Eucalyptus chlorophylla		Elaeocarpus arnhemicus			Pogonolobus reticulatus
Eucalyptus cloeziana		Erythrophleum			Sarcostemma viminale
Eucalyptus crebra		chlorostachys			Senna magnifolia
Eucalyptus cullenii		Erythroxylum ellipticum			Tinospora smilacina
Eucalyptus herbertiana		Excoecaria parvifolia			Wrightia saligna
Eucalyptus intermedia		Exocarpos latifolius			
Eucalyptus jensenii		Ficus aculeata			
Eucalyptus koolpinensis		Ficus scobina			
Eucalyptus leptophleba		Flindersia dissosperma			
Eucalyptus leptophylla		Gardenia ewartii			
Eucalyptus leucophloia		Gardenia fucata			
Eucalyptus lirata		Gardenia megasperma			
Eucalyptus melanophloia		Gardenia resinosa			
Eucalyptus microneura		Geijera parviflora			
Eucalyptus microtheca		Geijera salicifolia			
Eucalyptus miniata		Grevillea agrifolia			
Eucalyptus obconica		Grevillea angulata			
Eucalyptus orgadophila		Grevillea decurrens			
Eucalyptus patellaris		Grevillea dimidiate			
Eucalyptus persistens		Grevillea glauca			
Eucalyptus phoenicea		Grevillea heliosperma			
Eucalyptus platyphylla		Grevillea parallela			
Eucalyptus polycarpa		Grevillea pteridifolia			
Eucalyptus populnea		Grevillea pyramidalis			
Eucalyptus pruinosa		Grevillea refracta			
Eucalyptus quadricostata		Grevillea striata			
Eucalyptus rhodops		Hakea arborescens			
Eucalyptus similis		Lophostem onlactifluus			
Eucalyptus tectifica		Lophostemon lactifluus			
Eucalyptus tereticornis		Lophostemon suaveolens			

[1]Euc. Typically single- stemmed hardwood trees from the genus Eucalyptus and closely related genera of *Corymbia* and *Angophora*.

[2]Multi. Multi-stemmed hardwood (angiosperm) trees, including trees from the genus *Acacia*.

[3]Other-H. Other tree species that typically have single stems and relatively high wood density (mean 0.67 g cm^{-3}).

[4]Other-L. Other trees, namely conifers from the genera of Araucaria and Agathis, that typically have single stems and relatively low stem wood density (mean 0.40 g cm-3).

[5]Shrubs or small trees characterized by being relatively short (generally <2 m height) and typically multi-stemmed or highly branched.

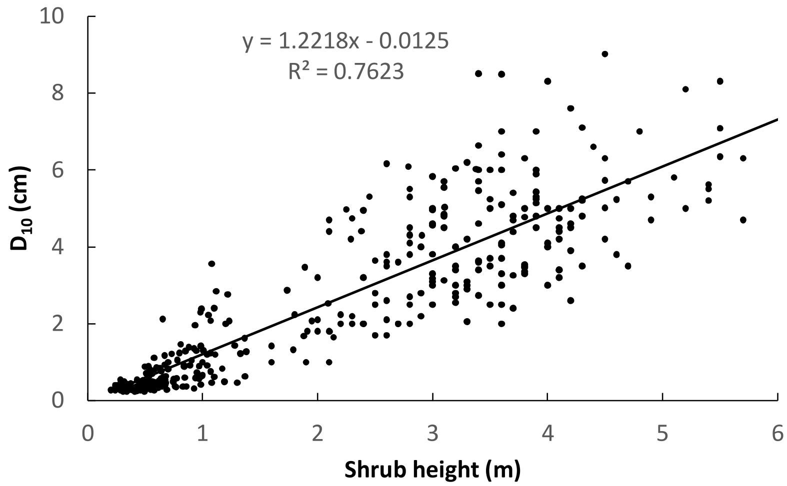

Fig. S7. Relationships between the height of a shrub (in m) and its stem diameter at 10 cm above the ground (D_{10}, in cm). These shrub datasets were described by Paul *et al.* (2016) and include only relatively small shrubs (<5 kg DM) from regions of relatively high mean annual rainfall (> 600 mm yr^{-1}).

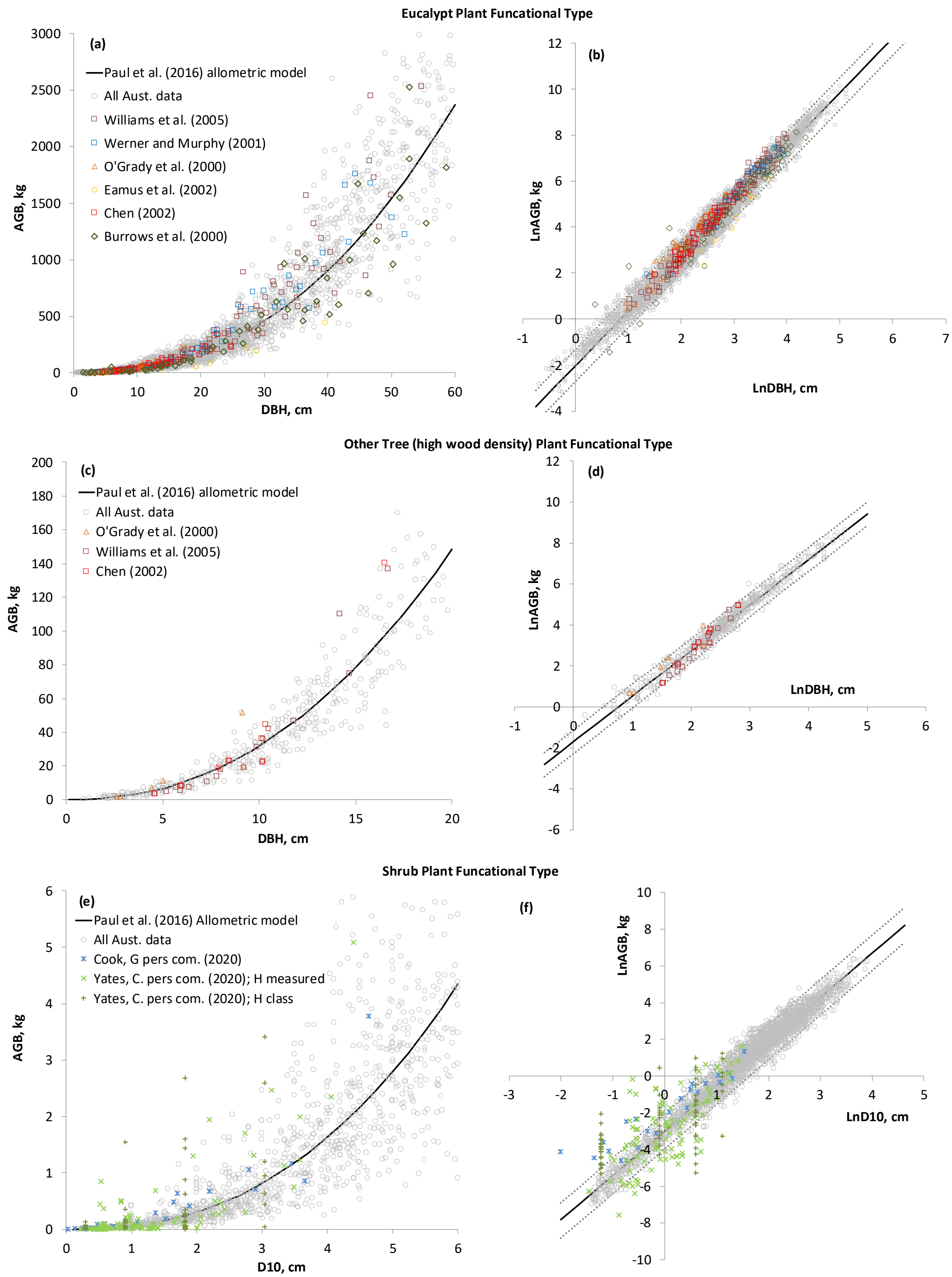

Fig. S8. Relationships between stem diameter and above-ground biomass (AGB, kg) of the PFTs: (a, b) Eucs, eucalypt trees; (c, d) Other-H, other trees of high wood density, and; (e, f) Shrubs. Data is expressed in both the natural scale (a,c,e) and the transformed scales (b,d,f). The Australian datasets and generic models are described by Paul *et al.* (2016). Black solid lines represent the model of best fit to the Australian dataset (grey symbols), while dotted lines the 95% prediction interval. Coloured symbols represent the datasets obtained from Australian savanna woodlands, many providing verification of the fitted allometric equations given they were independent dataset, with only the datasets of O'Grady *et al.* (2000) and Williams *et al.* (2005) used in the calibration of the allometric equation.

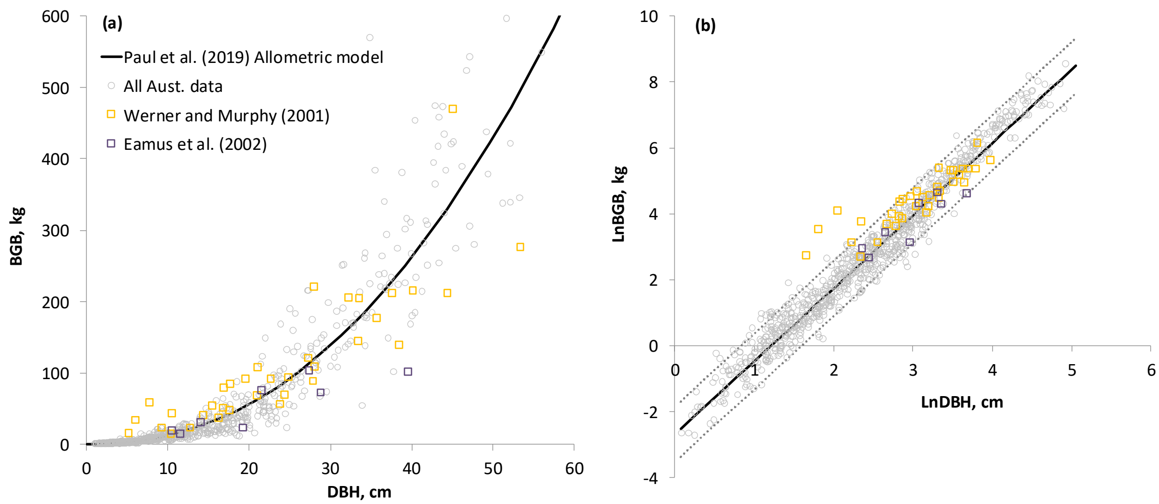

Fig. S9. Relationships between stem diameter and below-ground biomass (BGB, kg) of the plant functional type termed 'Other Trees' (i.e. all tree species with the exception of mallee eucalypts, acacias or shrubs). Data is expressed in both: (a) natural scale, and; (b) transformed scale. The Australian datasets and generic models are described by Paul *et al.* (2019). Black solid lines represent the model of best fit to the Australian dataset (grey symbols), while dotted lines the 95% prediction interval. Coloured symbols represent new independent datasets obtained from Australian savanna woodlands.

Table S3. Number of transects, transects size (ha), number of repeat measurements over time, and live above-ground biomass (AGB, Mg DM ha^{-1}). Averages are provided with ranges given in parenthesis. Data source: Murphy *et al.* (2023).

Region	Number of transects	Transects size (ha)	Number of repeat measurements	AGB* ($Mg\ DM\ ha^{-1}$)
Central Arnhem Land	96	0.085 (0.028-0.200)	5.6 (2-10)	32.6 (6.6-94.9)
Gulf of Carpentaria	162	0.109 (0.019-0.380)	7.5 (5-10)	27.0 (0-129.5)
Kakadu	60	0.078 (0.060-0.085)	4.3 (3-6)	47.6 (0-140.7)
Litchfield	30	0.080 (0.080-0.080)	5.0 (5-5)	43.8 (1.6-45.6)
Nitmiluk	36	0.080 (0.080-0.080)	5.0 (5-5)	30.5 (1.2-89.0)
Kimberley	68	0.134 (0.026-0.330)	5.9 (3-7)	19.7 (2.0-60.9)

*Murphy *et al.* (2023) monitored the stem diameters (D_{130}) of all live or dead trees and shrubs >5 cm D_{130} within 452 transects that together included 12,344 tagged trees or shrubs across six different regions of Australian savannas (Table S4). Each transect was surveyed between 2-10 times over a period of between 3-24 years, commencing in 1994 for the three large conservation reserves (Kakadu, Nitmiluk and Litchfield National Parks), and commencing in 2006 for the other three regions. Allometric equations were applied to estimate 'observed' AGB (Section 2.3) at each transect. These estimates will be under-estimates of the true AGB within these stands given, as outlined by Murphy *et al.* (2023): (i) trees or shrubs of D_{130} < 5 cm were excluded from the monitoring, with the exception of where a stem was observed to attain > 5 cm later; (ii) for multi-stemmed trees or shrubs, only the D_{130} of the main stem was tagged and monitored for changes in D_{130}, and; (iii) monocotyledons (e.g. palms) and other arborescent groups (e.g. cycads) were excluded from the monitoring.

Additional (not previously used) data from Australian savannas were sourced to provide verification of the allometric equations, with most of the independent measures of tree live AGB (Fig. S8) or BGB (Fig. S9) fitting within the 95% predictions intervals. Exceptions included some AGB data from shrubs, which may have been attributable to uncertainties in 'observed' D_{10}, given these were estimates. Nevertheless, it is also possible that the relatively high variation in AGB of shrubs, and also BGB of small trees, may be partly attributable to the relative frequency of fire-impacts on savanna shrubs and small trees when compared to shrubs in other regions of Australia where fire frequencies are much lower. This requires further investigation.

Heavy pools

Stag biomass was calculated through the application of stag-specific allometric equations (Fig. S10) applied to the trees or shrubs identified by technicians as being dead during the transect-based surveys of stem diameters (e.g., Murphy *et al.* 2023). Using the approach of Fensham (2005), to develop these stag-specific equations, a theoretical estimate of stag AGB was calculated for the

Paul *et al.* (2016) dataset using only the bole component of the observed live AGB, with the canopy component being excluded. The bole components included stem wood, bark and large branches of ca. 2-5 cm diameter that could easily be separated from the crown (foliage and twigs) by technicians using secateurs. Then, a multiplier of 1.399 was applied to convert observations of dry weights of live bole biomass into estimates of biomass of dead boles. This multiplier was based on the findings that dead biomass has significantly lower moisture contents (average 16% across 174 samples) than live biomass (averages 40% across 1,270 samples; Paul *et al.* 2017).

The PFT-based allometric models were of the form Bole (kg) = $v.D^w$, where D is the stem diameter (cm; either D_{10} or D_{130}, depending on the PFT), and parameters v and w were fitted to optimise the model efficiency of prediction. Model efficiency of prediction of bole biomass across the subset of Paul *et al.* (2016) dataset (i.e., for those where AGB components were separately measured) was between 72 and 86% (Fig. S10).

The stag component of heavy fuel was calculated through the application of stag-specific allometric equations applied to the trees or shrubs identified by technicians as being dead during the transect-based surveys of stem diameters (e.g., Murphy *et al.* 2023). The 452 stem-diameter transect surveys that were monitored for AGB (Table S3) were also monitored for stag biomass, i.e., the stem diameters of trees or shrubs that were deemed to be dead. An additional 171 transects had similar measurements of stag diameter (Table S4). Hence, in total 623 transect surveys were used to estimate the stand-level stag biomass. There were also 849 observations of CWD (Russell-Smith *et al.* 2009; Yates *et al.* 2015; Lynch *et al.* 2018), with these datasets indicating average CWD was significantly ($P>0.05$) higher in zones of savanna where rainfall was relatively high, e.g., WH *cf.* WL or SL (Table S5).

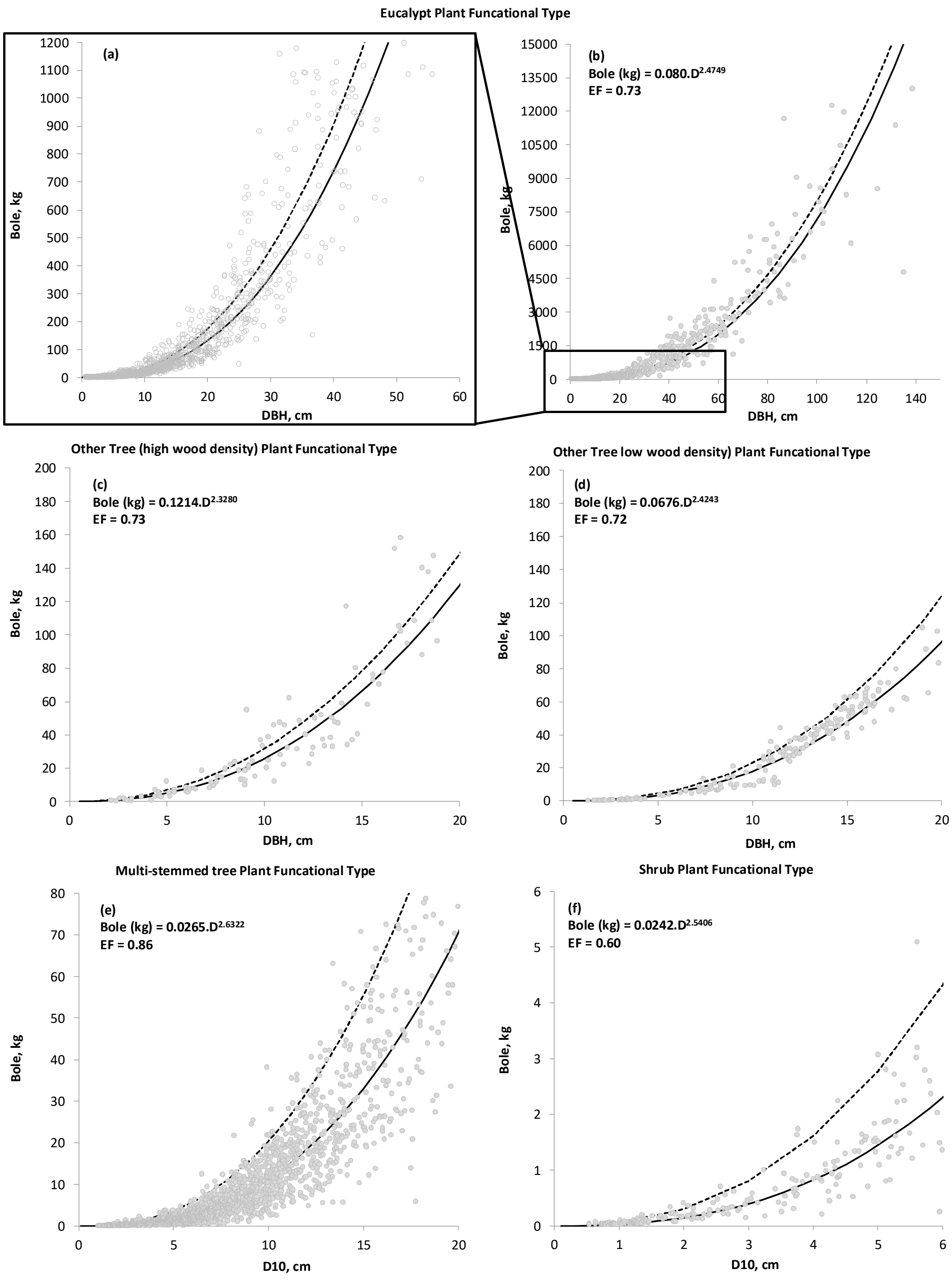

Fig. S10. Relationships between stem diameter and above-ground biomass of the bole components (Bole, kg) of the PFTs: (a, b) Eucs, eucalypt trees; (c) Other-H, other trees of high wood density; (d) Other-L, other trees of low wood density; (e) Multi, multi-stemmed trees (namely acacias), and; (f) Shrubs. The Australian datasets and generic models are described by Paul *et al.* (2016). Black solid lines represent the model of best fit to the Australian dataset (grey symbols), while to provide a reference, dotted lines represent the model of best fit to total AGB (i.e. Bole plus canopy components) observed for these trees or shrubs.

Table S4. Number of transects, transects size (ha), stand estimates of above-ground biomass of stags (standing dead trees or shrubs, Mg DM ha^{-1}). Averages are provided with ranges given in parenthesis.

Data source	Number of transects	Transect size (ha)	AGB (Mg DM ha^{-1})
Bray *et al.* (2014)	44	0.10-0.15	71 (6.1-291)
Lynch *et al.* (2018)	88	0.03-0.10	14 (0.0-70)
Cook *et al.* (2020)	15	0.20-2.00	32 (5.8-79)
Murphy *et al.* (2023)	452	0.02-0.38	30 (0.6-141)
Bray, S. pers com (2020)	24	0.05-1.20	47 (2.1-110)

Table S5. Number of transects, transects size (ha) and stand estimates of on-ground coarse woody debris (CWD) components of heavy fuel (Mg DM ha^{-1}). Averages and standard errors (s.e.) are provided, with ranges given in parenthesis. The groups with the same letters are not significantly different according to the Tukey analysis of differences between categories with a confidence interval of 95%. See Table 1 for explanation of vegetation types.

Vegetation type	Data source	N	CWD* (Mg DM ha^{-1})	s.e	Groups		
WH	Russell-Smith *et al.* (2009)	181	3.54 (0.00-30.7)	0.22	A		
PL	Lynch *et al.* (2018)	99	2.04 (0.00-16.3)	0.30		B	
SH	Russell-Smith *et al.* (2009)	50	1.68 (0.00-8.34)	0.42		B	C
WL	Yates *et al.* (2015)	488	1.15 (0.00-34.2)	0.13			C
SL	Yates *et al.* (2015)	31	0.29 (0.00-2.17)	0.53			C

*Sampling for CWD was undertaken in a 5 m × 100 m swath, recording the length, diameter and hollowness of all fuel sections >5 cm diameter. Assuming each piece was cylindrical in shape, total volume of CWD was estimates and then converted to a mass by assuming a specific gravity of 0.995 Mg DM m^{-3} (approximating that of eucalypt wood; Eamus *et al.* 2002).

Table S6. Observations of 'shrub' fuel (Mg DM ha^{-1}) within the various categories of savanna vegetation. Averages and standard deviations (s.d) are provided, with ranges given in parenthesis. The groups with the same letters are not significantly different according to the Fisher analysis of differences between categories with a confidence interval of 95%. See Table 1 for explanation of vegetation types.

Vegetation type	Data source	N	Average 'shrub' fuel biomass* (Mg DM ha^{-1})	s.d	Groups		
PL	Lynch *et al.* (2018)	102	5.91 (0.42-47.00)	5.70	A		
SH	Russell-Smith *et al.* (2009)	50	1.77 (0.16-15.08)	2.31		B	
WH	Russell-Smith *et al.* (2009)	189	1.16 (0.02-9.99)	1.49		B	C
SL	Yates *et al.* (2015)	13	1.01 (0.23-2.28)	0.65		B	C
WL	Yates *et al.* (2015)	374	0.80 (0.00-7.99)	1.15			C

*Shrub fuel was defined as woody vegetation with D_{130}< 5 cm.

Coarse, fine and grass fuel

As outlined in Tables S7-S9, there were 898, 1,356 and 1,060 observations of coarse, fine and grass fuel, respectively (Russell-Smith *et al.* 2009; Yates *et al.* 2015; Lynch *et al.* 2018; Yates *et al.* 2020). These datasets indicated that the average size of these pools varied (often statistically significantly) between categories of savanna vegetation, including their typical cover of woody-to-grass components. For example, as expected, coarse fuel biomass was relatively low for shrubland vegetation (SH and SL) (Table S7), while for vegetation in low rainfall zones (WL, and particularly SL), fine and grass fuel biomass was relatively low and high, respectively.

Table S7. Observations of coarse fuel biomass (Mg DM ha^{-1}). Averages and standard errors (s.e) are provided, with ranges given in parenthesis. The groups with the same letters are not significantly different according to the Tukey analysis of differences between categories with a confidence interval of 95%. See Table 1 for explanation of vegetation types.

Veg. type	Data source	N	Coarse fuel* (Mg DM ha^{-1})	s.e	Groups	
PL	Lynch *et al.* (2018)	101	1.62 (0.07-7.85)	0.12	A	
WH	Russell-Smith *et al.* (2009)	189	1.23 (0.03-5.61)	0.09	A	B
WL	Yates *et al.* (2015)	551	0.90 (0.00-11.7)	0.05	A	B
SL	Yates *et al.* (2015)	7	0.73 (0.05-2.47)	0.46		B
SH	Russell-Smith *et al.* (2009)	50	0.58 (0.00-2.29)	0.17		B

*The biomass of coarse fuel was estimated from sampling the fresh weight of twigs and bark (diameter 0.6-5 cm) within 1 × 1 m quadrants at 10 m intervals along 100 m transects. Sub-samples were taken for moisture content determination to convert fresh weight to dry weight.

Table S8. Observations of fine fuel biomass (Mg DM ha^{-1}). Averages and standard errors (s.e.) are provided, with ranges given in parenthesis. The groups with the same letters are not significantly different according to the Tukey analysis of differences between categories with a confidence interval of 95%. See Table 1 for explanation of vegetation types.

Veg. type	Data source	N	Fine fuel* (Mg DM ha^{-1})	s.e	Group			
PL	Lynch *et al.* (2018)	102	3.45 (0.11-22.8)	0.17	A			
WH	Russell-Smith *et al.* (2009); Yates *et al.* (2020)	296	2.54 (0.02-12.8)	0.10		B		
SH	Russell-Smith *et al.* (2009)	47	1.91 (0.02-7.01)	1.91		B	C	
WL	Yates *et al.* (2015, 2020)	778	1.54 (0.00-13.9)	1.54			C	
SL	Yates *et al.* (2015)	133	1.06 (0.02-8.13)	1.06				D

*Biomass of fine fuel was estimated from sampling the fresh weight of foliage and bark litter (diameter <0.6 cm) as well as grass from within a 1 × 1 m quadrant at 20 m intervals along 100 m transects. Sub-samples were taken for moisture content determination to convert fresh weight to dry weight.

Table S9. Observations of grass fuel biomass (Mg DM ha^{-1}). Averages and standard errors (s.e.) are provided, with ranges given in parenthesis. The groups with the same letters are not significantly different according to the Tukey analysis of differences between categories with a confidence interval of 95%. See Table 1 for explanation of vegetation types.

Veg. type	Data source	N	Grass fuel* (Mg DM ha^{-1})	s.e	Group		
SL	Yates *et al.* (2015)	133	2.21 (0.00-8.82)	0.12	A		
$WL_{0.1}$	Yates *et al.* (2015, 2020)	486	2.12 (0.00-15.1)	0.06	A		
$WL_{0.2}$	Yates *et al.* (2015, 2020)	292	1.52 (0.00-6.67)	0.08		B	
SH	Russell-Smith *et al.* (2009)	47	1.47 (0.02-5.31)	0.20		B	
PL	Lynch *et al.* (2018)	102	1.29 (0.07-4.50)	0.13		B	
$WL_{0.3}$	Russell-Smith *et al.* (2009); Yates *et al.* (2020)	155	1.16 (0.02-6.59)	0.11		B	C
$WL_{0.6}$	Russell-Smith *et al.* (2009); Yates *et al.* (2020)	141	0.73 (0.00-3.74)	0.11			C

*Biomass of fine fuel was estimated from sampling the fresh weight of foliage and bark litter (diameter <0.6 cm) as well as grass from within a 1 × 1 m quadrant at 20 m intervals along 100 m transects. Sub-samples were taken for moisture content determination to convert fresh weight to dry weight.

Because vegetation types of differing typical woody fractional covers may have different grass biomass (Thackway *et al.* 2014; Lynch *et al.* 2018), vegetation categories of WH and WL were sub-divided into sub-categories of differing woody fractional covers for simulation of grass fuel (Table S1). With this exception, the broader vegetation categories were sufficient to explain typical differences in fuel pool sizes when applying previously used fine-level categorisation of savanna vegetation *cf.* to these broader categories (Table 1), only an additional 3-6% of variation in observed fuel pool sizes was explained, and with no apparent reasons for this (Tables S10a-d).

Table S10a. Average and standard error estimates of coarse woody debris (CWD) components (Mg DM ha^{-1}). The groups with the same letters are not significantly different according to the Tukey analysis of differences between categories with a confidence interval of 95%. See Table 1 for explanation of vegetation types and how these relate to the broader categorisation of savanna vegetation applied in this study.

Vegetation type	Average (Mg DM ha^{-1})	s.e	Groups			
hOFM	4.928	0.315	A			
hWHu	2.878	0.460		B		
Pindan	2.042	0.289		B	C	
hWMi	2.026	0.374		B	C	
lWMi	2.017	0.310		B	C	
hSHH	1.681	0.406		B	C	D
lWTu	1.248	0.269		B	C	D
lWHu	1.145	0.443			C	D
lOWM	0.803	0.183			C	D
lSHH	0.290	0.516				D

Table S10b. Average and standard error (s.e) estimates of coarse fuel (Mg DM ha^{-1}). The groups with the same letters are not significantly different according to the Tukey analysis of differences between categories with a confidence interval of 95%. See Table 1 for explanation of vegetation types and how these relate to the broader categorisation of savanna vegetation applied in this study.

Vegetation type	Average (Mg DM ha^{-1})	s.e	Groups		
lWHu	1.854	0.190	A		
Pindan	1.623	0.118	A	B	
hOFM	1.453	0.125	A	B	C
lWTu	1.389	0.132	A	B	C
hWHu	1.168	0.190	A	B	C
hWMi/hWTu	0.937	0.153		B	C
lSHH	0.728	0.448			C
lOWM	0.724	0.062			C
lWMi	0.691	0.144			C
hSHH	0.576	0.168			C

Table S10c. Average and standard error (s.e.) estimates of fine fuel (Mg DM ha^{-1}). The groups with the same letters are not significantly different according to the Tukey analysis of differences between categories with a confidence interval of 95%. See Table 1 for explanation of vegetation types and how these relate to the broader categorisation of savanna vegetation applied in this study.

Vegetation type	Average (Mg DM ha^{-1})	s.e	Groups					
Pindan	3.451	0.166	A					
hOFM	2.888	0.142	A	B				
hWHu	2.530	0.204	A	B	C			
hWMi/hWTu	2.486	0.217	A	B	C			
lWTu	2.450	0.174	A	B	C			
lWHu	2.167	0.259		B	C	D		
lWMi	1.954	0.143		B	C	D	E	
hSHH	1.913	0.245		B	C	D	E	F
Other	1.678	0.396			C	D	E	F
lOWM	1.193	0.076				D	E	F
lSHH	1.058	0.146					E	F
hWMi	0.901	0.324						F

Table S10d. Average and standard error (s.e.) estimates of grass fuel (Mg DM ha^{-1}). The groups with the same letters are not significantly different according to the Tukey analysis of differences between categories with a confidence interval of 95%. See Table 1 for explanation of vegetation types and how these relate to the broader categorisation of savanna vegetation applied in this study.

Vegetation type	Average (Mg DM ha^{-1})	s.e	Groups			
lSHH	2.207	0.115	A			
lWHu	2.168	0.205	A			
lOWM	2.118	0.060	A			
lWTu	1.939	0.138	A	B		
Other	1.609	0.314	A	B	C	
hWMi	1.493	0.256	A	B	C	D
hSHH	1.472	0.194	A	B	C	D
Pindan	1.286	0.132		B	C	D
hWMi/hWTu	1.212	0.172		B	C	D
lWMi	1.043	0.113			C	D
hWHu	0.981	0.161			C	D
hOFM	0.729	0.112				D

Additional Tables and Figures relating to allocation and litterfall

Table S11. Collated Australian savanna dataset of allocation of total AGB to components of stem (Stem:AGB), branches (Branch:AGB), bark (Bark:AGB), and foliage (Foliage:AGB) for the plant functional types of Eucalypts (Euc), Other trees of high wood density (Other-H), and shrubs (Shrub). Definitions of these plant functional types, and a list of species found in savanna vegetation that were allocated to these, is provided in Table S2.

PFT	Source	Stem:AGB	Branch:AGB	Bark:AGB	Foliage:AGB
Euc	O'Grady *et al.* (2000)	0.604	0.240	0.118	0.037
	Werner & Murphy (2001)	0.652*	0.121	0.197*	0.032
	Chen (2002)	0.543	0.260	0.137	0.040
	Eamus *et al.* (2002)	NA	NA	NA	0.051
	Average	***0.602***	***0.207***	***0.151***	***0.040***
Other-H^	Chen (2002)	0.522	0.183	0.240	0.057
	Average	***0.522***	***0.183***	***0.239***+	***0.057***
Shrub^	Yates, C. pers comm.	0.210*	0.379	0.081*	0.330
	Yates, C. pers comm.	NA	NA	NA	0.377
	Cook, G. pers comm.	NA	NA	NA	0.439
	Average	***0.210***	***0.379***	***0.029***+	***0.382***

*Bark measured together with stem, and thus stem and bark components were estimates by assuming the proportion of the total stem plus bark component that was stem was 0.799 and 0.721 for Euc and Shrub, respectively. This estimate was based on allocation measured by O'Grady *et al.* (2000) and Chen (2002) for savanna eucalypts, and for shrubs from southern regions of Australia.
+Estimates of average Bark:AGB were adjusted from that observed to ensure that the total allocation added to 1.000 across all pools of AGB. The bark component was adjusted as it was assumed to be more uncertain than stem, branch or foliage allocation.
^Given there were no data available for Multi and Other-L, it was assumed AGB allocation for these PTF was the same as observed for Shrub and Other-H, respectively.

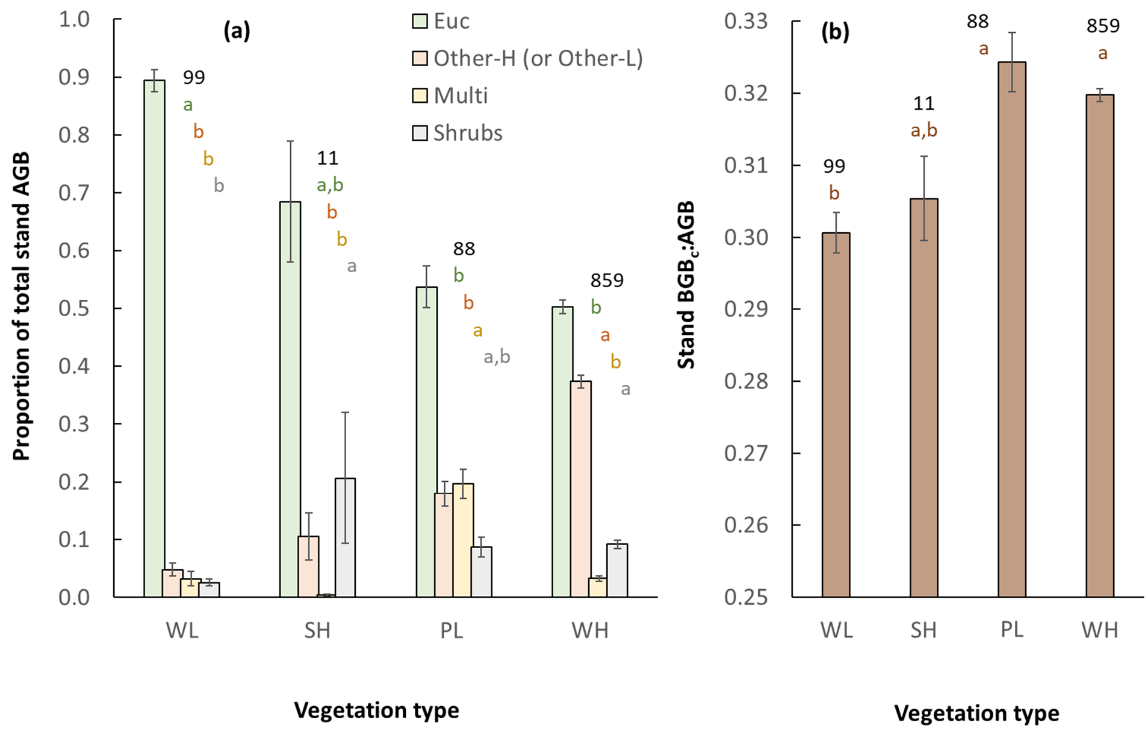

Fig. S11. Summary of allocation of live biomass to components derived from interrogation of the 1,091 transect-based stand biomass surveys of WL, SH, PL and WH savanna vegetation, including: (a) proportion of total stand AGB that is allocated to the various plant functional types, and (b) ratio of coarse root biomass to above-ground biomass (BGB_C:AGB). Error bars represent the standard error of the mean. Numbers above the bars represent the replicate number of stands (N) representing the category of vegetation. Data source: Stem diameter inventories (Tables S3 and S4) , with the application of verified PFT-based allometric models (Paul *et al.* 2016, 2019). Based on their location, these stands were categorised into the different savanna vegetation types. However, to ensure that stands found within the regions deemed to be SL or SH were actually shrublands, stands were only categorised as these vegetation types if they had >10% of the individuals surveyed being of the Shrub plant functional type. Based on the Tukey test, categories with the same letters above the bar are not statistically different from one another at a confidence limit of 95%, with green, orange, yellow, grey and brown letters indicating the results for PropEuc, PropOther, PropMulti, PropShrub and BGB_C:AGB, respectively.

Table S12. Average observed litterfall (Mg C ha^{-1} yr^{-1}) in Australian savannas in high and low rainfall zones, with ranges given in parenthesis. The carbon concentration of biomass collected in litter traps was assumed to be 48%.

Rainfall zone	Data source	N	Litterfall* (Mg C ha^{-1} yr^{-1})
High	Yates *et al*. (2020)	24	1.09 (0.09-3.96)
	Cook (2003)	8	2.12 (1.60-2.69)
	Chen (2002); Chen *et al.* (2003)	1	0.82
	Finlayson *et al.* (1988; 1993)	2	3.42 (3.39-3.45)
	Cuff & Brocklehurst (2015)	9	2.67 (1.69-3.65)
Low	Cuff & Brocklehurst (2015)	9	1.36 (0.85-2.29)
	McIvor (2001)	2	0.48 (0.35-0.62)
	Yates *et al*. (2020)	6	0.76 (0.36-1.38)

*Litter accumulated in litter traps (e.g., 1 x 1 m steel frame with flyscreen mesh raised about 1 m the ground) was monitored within 61 stands from across the high and low rainfall regions of Australian savannas.

Additional calculations required to constrain turnover parameters

Although there were 61 savanna stands that had litterfall datasets, two additional calculations were required to use these observations to derive estimates for component of biomass simulated by FullCAM. Firstly, estimates of total litterfall attributable to foliage, branch and bark required estimation. To do this, data was utilised from a sub-set of litterfall studies that separated out components (Finlayson *et al.* 1993; McIvor 2001; Cuff and Brocklehurst 2015; Yates *et al.* 2020), where it was found branches and bark typically comprise only 9% ± 8% (N=33) and 6% ± 3% (N=3) of observed (average ± standard deviation) biomass collected from litter traps, respectively. Second, a multiplier was required to convert litterfall measured from litterfall traps into total litterfall given these traps often fail to capture spatially heterogenous litterfall arising from large branches (and pieces of bark, and any twigs or foliage attached to these larger branches) due to only about 0.003 ha of the stand typically being monitored (= 0.0001 ha trap area × 30 replicates). By monitoring traditional litterfall traps as well as the accumulation of large litter (≥ 0.6 cm) within savanna areas of 0.04 ha (= 0.0025 ha quadrant area × 15 replicates), Yates *et al.* (2020) found that for the 30 stands monitored, additional turnover attributable to larger components of litter averaged (± standard deviation) 33% ± 22% (range 6-79%). Based on these results, for a stand of any given

AGB, total input of carbon due to turnover was expected to be about 1.33 times the litterfall observed using traditional litter traps. Here it was assumed that this additional litterfall was comprised of only branches (60%) and bark (40%), with no contribution from foliage. This meant that the assumed proportion of *total* litterfall (trap + additional) attributable to branch and bark was 22% and 15%, respectively.

SM-D: Additional Tables and Figures to explain scenarios of fire management

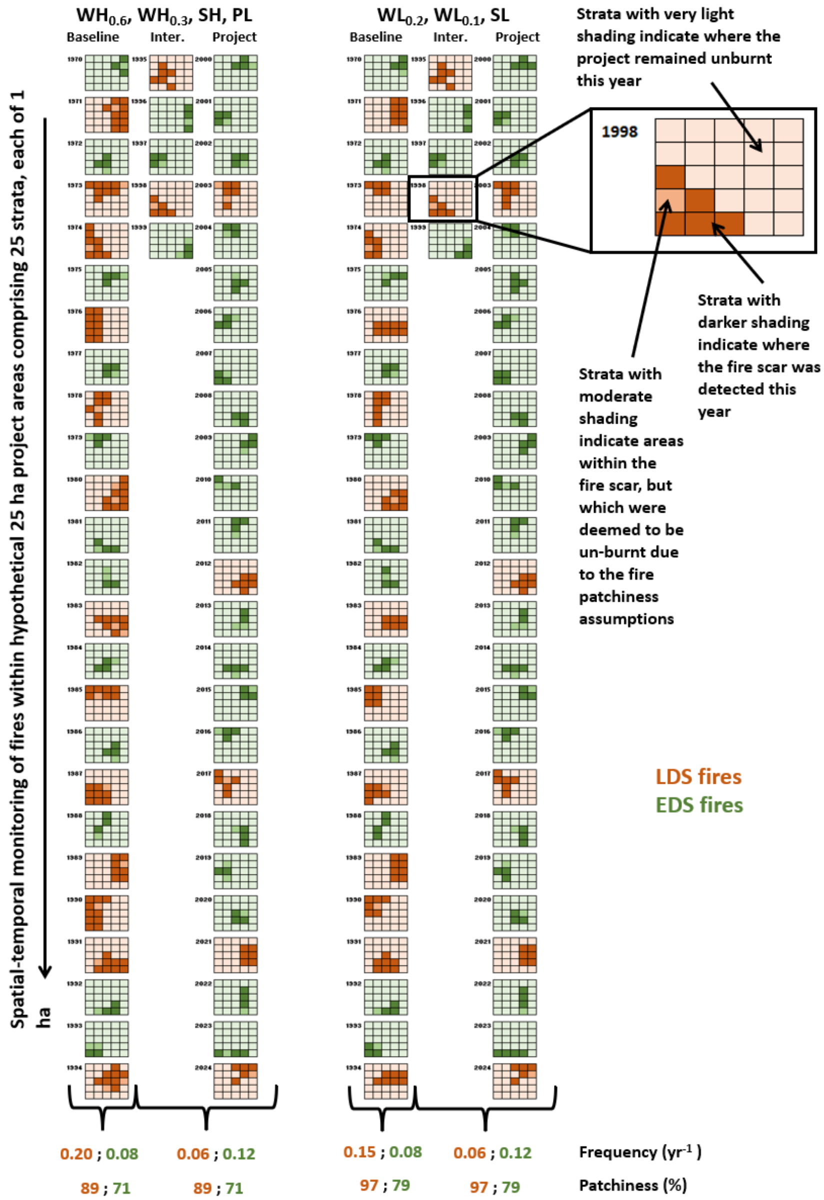

Fig. S12. Hypothetical savanna burning project areas in regions where the baseline fire frequency was assumed to be either relatively high ($WH_{0.6}$, $WH_{0.3}$, SH and PL), or relatively low ($WL_{0.2}$, $WL_{0.1}$, and SL). Scenarios entailed simulation of a hypothetical 25 ha project area containing 25 × 1 ha strata, with each strata having different fire histories. Simulations entailed a 25-year baseline period followed by a 5-year intermediate period where fire management commences and pools of carbon begin to re-equilibrate, and then a subsequent 25-year project period. Average frequencies of LDS_2 and EDS_2 fires across the project-area was assumed to change between the baseline and project period as indicated. Results from this scenario analysis are shown in Fig. 8.

Table S13. The assumed maximum above-ground biomass (M, Mg DM ha^{-1}) for each category of savanna vegetation, based on the average observed across the calibration sites for these vegetation types (Fig. 2).

Vegetation category	Assumed location (decimal degrees)	Assumed M (Mg DM ha^{-1})
$WH_{0.6}$	-12.7; 132.0	99
$WH_{0.3}$	-12.7; 132.0	47
SH	-12.7; 132.0	13
PL	-17.0; 122.7	28
$WH_{0.2}$	-17.5; 138.4	35
$WH_{0.1}$	-17.5; 138.4	19
SL	-17.5; 138.4	3

SM-E: Relative sensitivities of different savanna vegetation types to fire

When considering the relative sensitivity of different savanna vegetation types to fire, some insights can be gained from the average proportion of total woody biomass that is heavy fuel, and from the average proportion of AGB that is deemed to be combusted by fire, e.g., proportion of the total stand AGB attributable to smaller fire-impacted PFTs such as shrubs. Across the different categories of savanna vegetation, the average observed proportion of total woody biomass that was heavy fuel was found to increase with increasing average proportion of maximum AGB (i.e. *M*) that was 'shrub' fuel (Fig. 13a). Shrublands (SH and SL) tend to have the highest 'shrub' fuel biomass as a proportion of AGB (Fig. S11), and thus, have relatively high proportions of heavy fuel. Because shrublands tend to have a relatively small biomass when compared to woodlands, this results in the average proportion of total woody biomass that is heavy fuel increasing with decreasing maximum AGB (Fig. 13b).

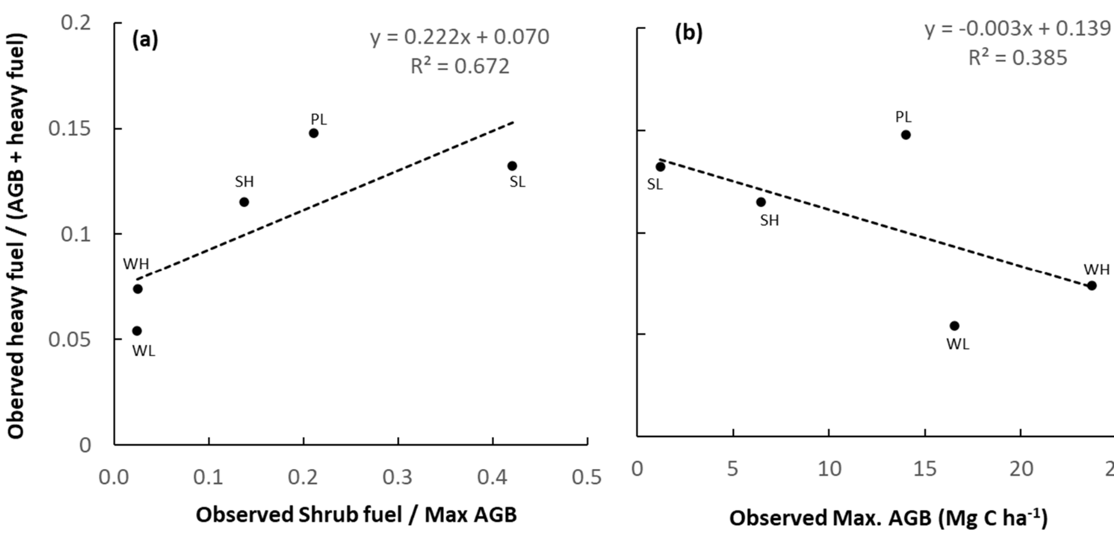

Fig. S13. Relationship between the observed heavy fuel as proportion of total woody biomass (including the live AGB and the dead heavy fuel) and: (a) observed proportion of maximum AGB that is 'shrub' fuel biomass (Table S5), and; (b) observed maximum AGB (Mg C ha^{-1}).

New analysis from the Territory Wildlife Park fire experiment (Levick *et al.* 2019) provided further evidence that smaller trees and shrubs that are predominately impacted by fire. This study showed that in contrast to larger trees, for the small woody components of the stand (i.e., trees and shrubs with < 2 m height and/or D_{130} < 3 cm), the contribution of stags to woody biomass (stag / (AGB + stag)) tended to increase with increasing fire frequency and intensity (Fig. S14).

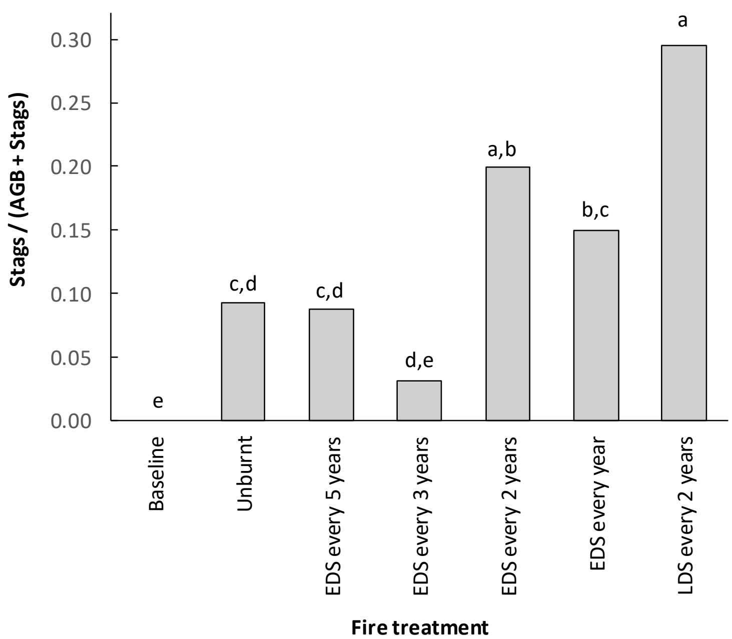

Fig. S14. For the small woody components of the stand (i.e., trees and shrubs with < 2 m height and/or D_{130} < 3 cm), observed proportion of stand woody biomass that was stags (stags / (AGB + stags)) in the baseline (i.e., prior to fire treatment implementation and following a prolonged period of no fires) and following 2-8 years of implementation of fire treatments with different frequencies and severities at the Territory Wildlife Park, described by Levick *et al.* (2019), and with datasets provided by Richards, A., Cook, G., Schatz, J. (pers. com). Bars with the same letters were not statistically different from one another according with the Tukey test at 95% confidence interval.

Additional figures

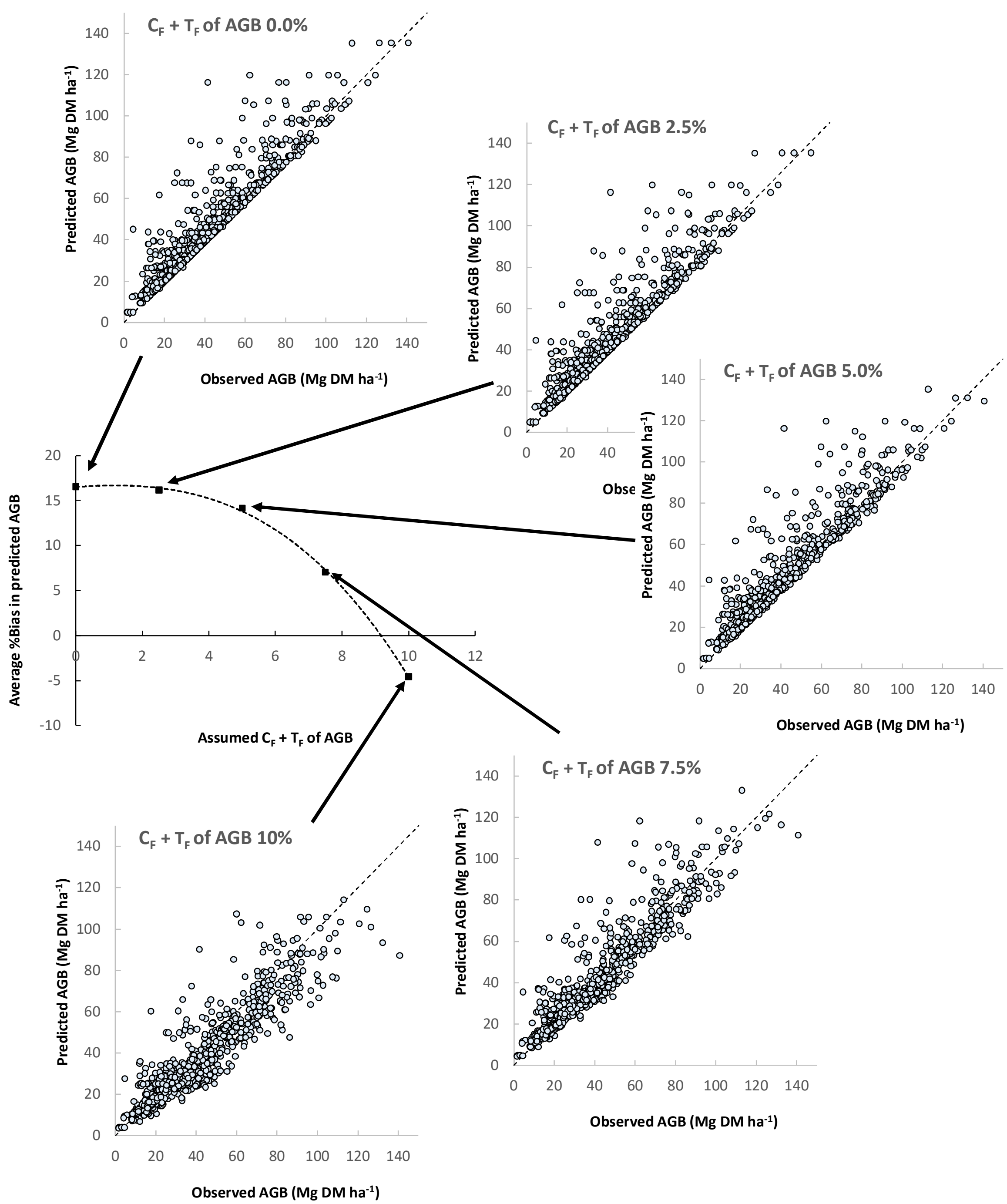

Figure S15. Relationship between the assumed total fire impact (C_F) on AGB and the average percentage bias in predicted stand AGB for the WH category of vegetation (N=1,103 stands). The average percentage bias attained with the calibration parameters for the WH vegetation (Table 3) was only 11.65%.

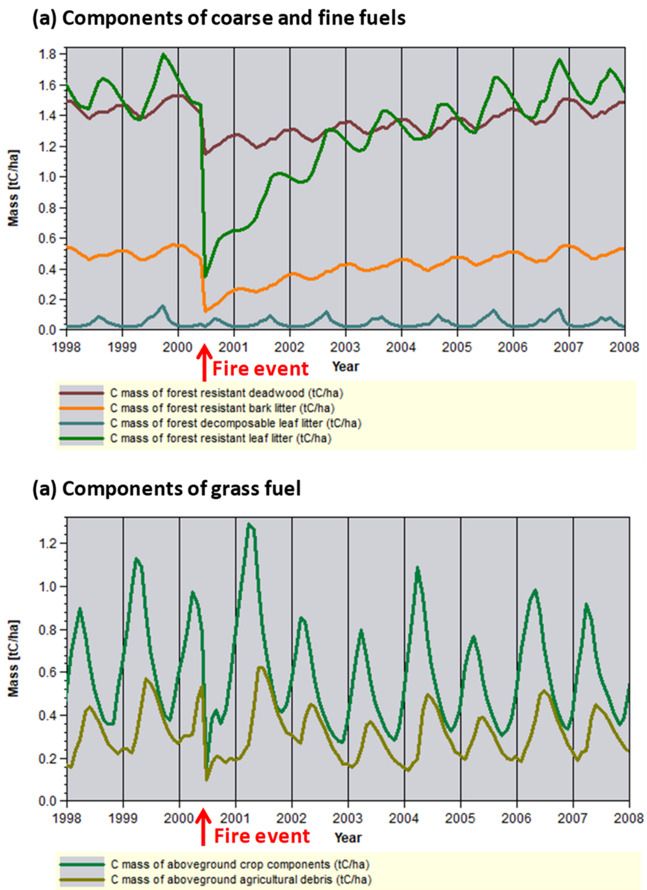

Fig. S16. FullCAM simulation of one example fire EDS2 event in a simulated WH stand. Outputs include: (a) components of coarse and fine fuels, including the resistant branch litter (or deadwood), resistant bark litter and also the decomposable and resistant components of foliage litter, and; (b) components of grass fuel, including the grass foliage (or above-ground biomass) and the grass litter (or above-ground debris).

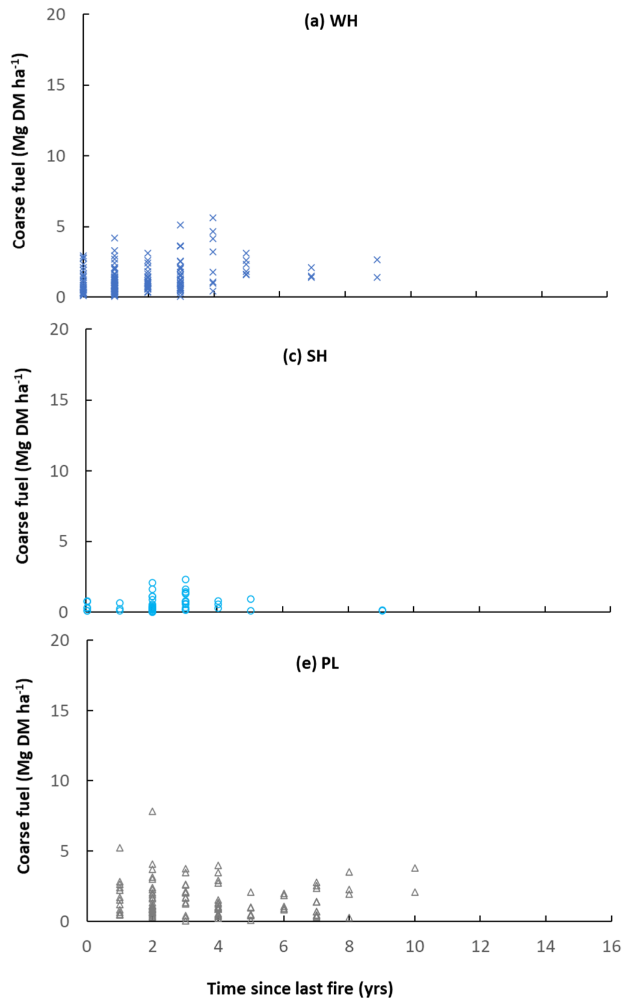

Fig. S17a. Observations of coarse fuel biomass (Mg DM ha^{-1}) expressed relative to the time since last fire (years) for: (a) WH; (b) WL; (c) SH; (d) SL, and (e) PL vegetation types. Source of data is given in Table S6. ANCOVA analysis indicated there was no statistically significant relationship between coarse fuel biomass and time since fire.

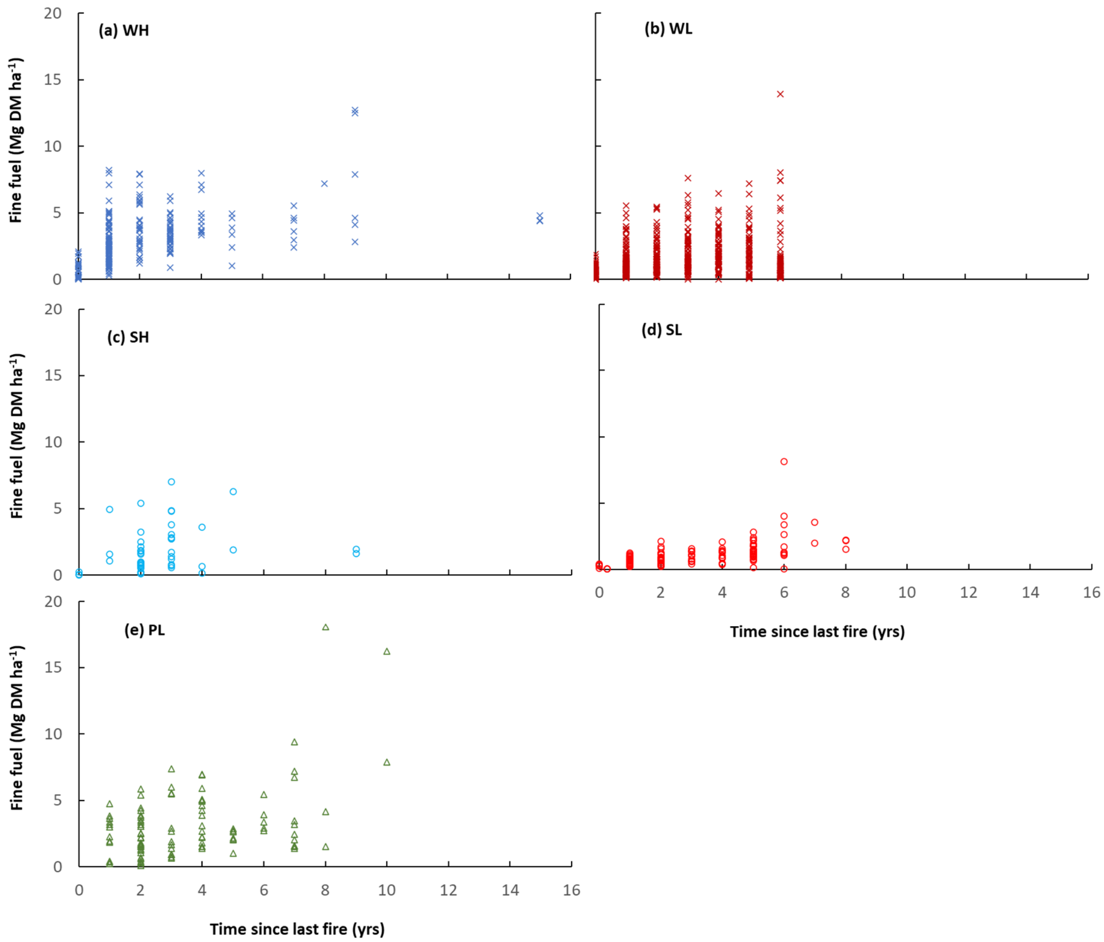

Fig. S17b. Observations of fine fuel biomass (Mg DM ha^{-1}) expressed relative to the time since last fire (years) for: (a) WH; (b) WL; (c) SH; (d) SL, and; (e) PL vegetation types. Source of data is given in Table S7. ANCOVA analysis confirmed that time since last fire contributed to explained variations in fine fuel amongst the different vegetation types (P<0.05).

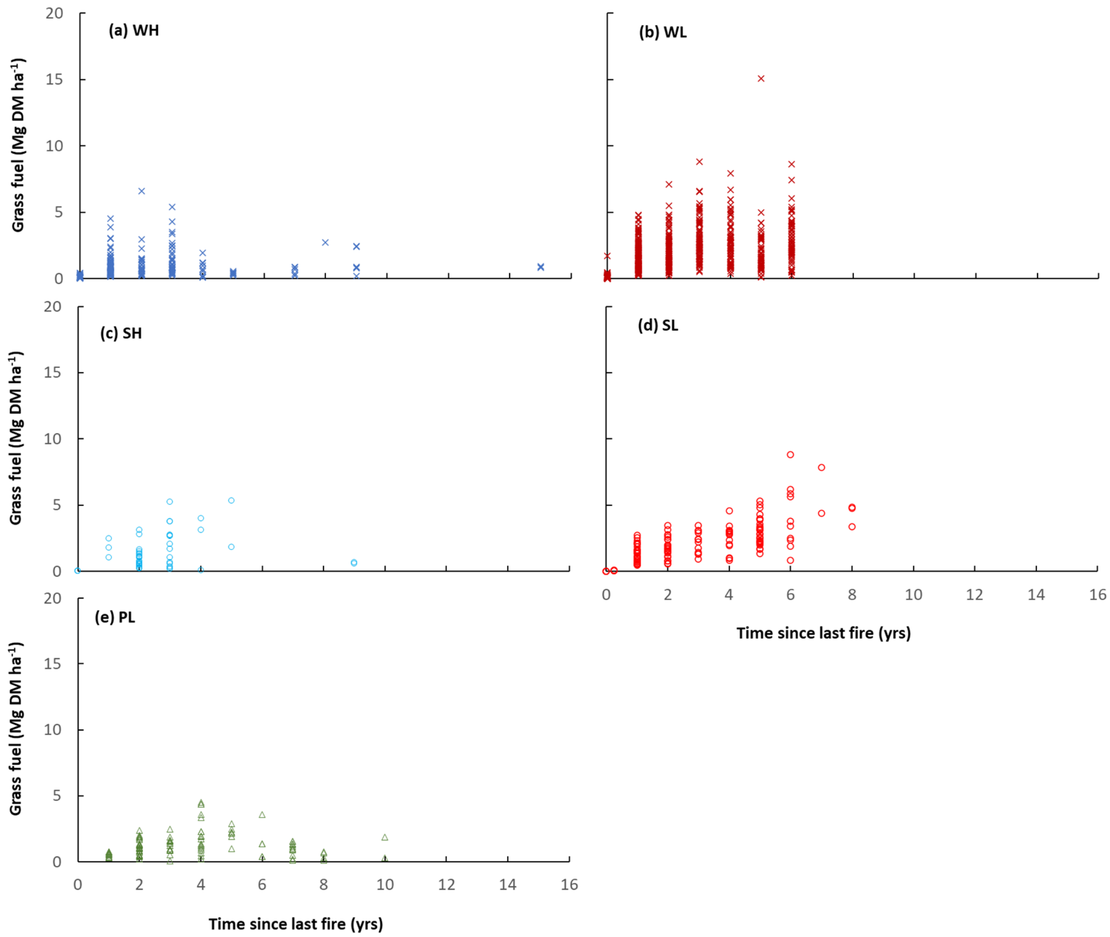

Fig. S17c. Observations of grass fuel biomass (Mg DM ha^{-1}) expressed relative to the time since last fire (years) for: (a) WH; (b) WL; (c) SH; (d) SL, and; (e) PL vegetation types. Source of data is given in Table S8. ANCOVA analysis confirmed that time since last fire contributed to explained variations in grass fuel amongst the different vegetation types ($P<0.05$).

SM-F: Opportunities for further improvements

Results from Fig. 8 indicated that sequestration of carbon in live biomass is a key driver of abatement following savanna fire management. These predictions are highly sensitive to the assumed upper limit of AGB, or the *M* input layer. Although verified for savanna vegetation (Fig. S2), the *M* input layer remains a key source of uncertainty given not all categories of savanna vegetation were represented in the calibration of this input layer (e.g., Pindan). Furthermore, fine-scale spatial variability found in savanna landscapes (e.g., due to variations in landscape position and soil type) are not accounted for in the *M* input layer. Given the emergence of high-resolution satellites and UAV LiDAR for monitoring of woody canopy cover (e.g., Guerschman *et al.* 2009; Pasut *et al.* 2023), an alternative approach may be to apply this satellite time-series cover data to directly monitor 'observed' AGB via application of empirical stand-based relationships between woody cover and AGB for the various categories of savanna vegetation.

This new approach would be another 'step-change' in the capability of FullCAM-predicted carbon dynamics in savannas, and would have the added advantage of: (i) informing estimates of changes to grass fuel biomass via assumed changed in productivity of grass related to changes observed in the monitored woody cover, (ii) avoiding uncertainty associated with the assumption that *M* represents the upper limit of AGB (Roxburgh *et al.* 2019), (iii) providing insights via satellite monitoring where 'observed' declines in cover and AGB cannot be reconciled with fire scar monitoring, and hence, are deemed non-fire related (e.g. die-back associated with severe drought periods (Fensham and Holman, 1999, Fensham and Fairfax, 2007, Fensham *et al.*, 2009, 2017) or cyclones (e.g., Hutley *et al.* 2013; Whitehead *et al.* 2022). Any on-going improvements in understanding of non-fire related impacts on AGB allows for improvements in understanding of fire-impact on AGB, and interactions between these. For example, the extent of fire-induced death of AGB will be attributable to interactions with termite attack, lightning strike and windthrow in high rainfall zones (Lonsdale and Braithwaite, 1991), and water stress due to competition during the late dry season in low rainfall zones (Cook *et al.* 2002; Liedloff and Cook 2007; Murphy *et al.* 2015).

A large amount of data was collated to constrain the calibration of model parameters. Despite this, many of these calibrations are highly uncertain due to the paucity of available data, e.g., rates of decomposition of pools of standing dead and debris. Parameters that could not be constrained due to negligible available data (mortality, C_F and T_F of AGB) were optimised in this study, and further work is required to verify these, and where required, constrain them to collected datasets.

There are three main areas where further improvements could be made to improve the accuracy of prediction of emissions from savanna fires. First, CF_s calibrations could be improved if informed by data that was specific to each component of fuel rather than from the observations based on previously defined categories of fuel (Meyer and Cook 2015). Second, given FullCAM simulates fires of differing intensity and predicts the composition of fuel, it may be possible to undertake further work to expand the capability of FullCAM to improve the accuracy of non-CO_2 gas fire emissions such that rather than being based on estimates vegetation type (a surrogate for these factors) they are calculated directly in accordance with fire intensity and fuel composition. This would enable predicted emissions from fire to vary in space and time, not just due to variations in FullCAM-predicted fuel loads, but also due to variations in FullCAM-predicted emission factors and the N:C ratios. Third, although patchiness of fires is based on rainfall zone and season, patchiness of a fire may also be influenced by the fuel load (e.g., Cook *et al.* 2017). There is now capacity to relate patchiness to the FullCAM-predicted fuel loads at a given stand at the time of the fire event.

In terms of application of FullCAM, further work is also required to generate high resolution spatial-temporal inputs of: (a) fire scars, and (b) fire severity. Currently, when FullCAM is applied in the NIR, fire scars are monitored using Advanced Very High-Resolution Radiometer (AVHRR, resolution of 1.1 km) given the temporal limitations of the lower saturation level (improved detection of less intense EDS fires) Moderate Resolution Imaging Spectrometer (MODIS, resolution of 1 km, but only available since 1999) data (Maier and Russell-Smith 2012). Until further work is completed to facilitate spatial-temporal fire severity data for Australian savannas (e.g., Edwards *et al.* 2018), when FullCAM is applied in the NIR, the simplifying assumption is made that all fires are either EDS_2 or LDS_2.

References

Anderson AN, Cook GD, Williams RJ (2003) Synthesis: Fire ecology and adaptive conservation management. In: Fire in Tropical Savannas : the Kapalga Experiment. Eds. Andersen, Alan N.; Cook, G. D.; Williams, R. J., New York: Springer; 2003. 153-164.

CoA (2022). National Greenhouse Gas Inventory Report: 2021. Australian Government submission to the United Nations Framework Convention on Climate Change and its first report under the Paris Agreement. Australia's National Greenhouse Accounts. Department of Climate Change, Energy, the Environment and Water, Canberra, Australia. Available at: https://www.dcceew.gov.au/climate-change/publications/national-inventory-report-2021

Bond WJ, Cook GD, Williams RJ (2012) Which trees dominate in savannas? The escape hypothesis and eucalypts in northern Australia. *Australia Ecology* **37**, 678-385.

Beringer J, Hutley LB, Tapper NJ, Cernusak LA (2007) Savanna fires and their impacts on net ecosystem productivity in North Australia. *Global Change Biology* **13**, 990-1004.

Bray S, Doran-Browne N, Reagain P (2014) Northern Australian pasture and beef systems. 1. Net carbon position. *Animal Production Science* **54**, 1988-1994.

Chen X (2002) Carbon balance of a eucalypt open forest savanna of northern Australia. PhD Thesis. Northern Territory University, Darwin.

Chen X, Hutley LB, Eamus D (2003) Carbon balance of a tropical savanna in northern Australia. *Oecologia* **137**, 405-416.

Cook GD, Williams RJ, Hutley LB, O'Grady AP, Liedloff AC (2002) Variation in vegetative water use in the savannas of the North Australian Tropical Transect. *Journal of Vegetation Science* **13**, 413-418.

Cook GD (2003) Fuel dynamics, nutrients and atmospheric chemistry. In 'Fire in tropical savannas: the Kapalga experiment'. (Eds AN Andersen, GD Cook, RJ Williams) pp. 47–58. (Springer: New York, NY, USA)

Cook GD, Goyens CMAC (2008) The impact of wind on trees in Australian tropical savannas: lessons from the impact of Cyclone Monica. *Austral Ecology* **33**, 462 - 470.

Cook GD, Liedloff AC, Murphy BP (2015) Towards a methodology for increased carbon sequestration in dead fuels through implementation of less severe fire regions in savannas. "Carbon Accounting and Savanna Fire Management", Eds: Brett P. Murphy, Andrew C. Edwards, Mick Meyer and Jeremy Russell-Smith, CSIRO Publishing, Clayton South, Victoria, Australia, pp 321-326.

Cook GD, Meyer CP, Richards AE, Liedloff AC, Schatz CJ (2017) Carbon sequestration resulting from management of fires on the Tiwi Islands: Progress Report 31 March 2017. CSIRO, Australia.

Cook GD, Liedloff AC, Meyer CP, Richards AE, Bray SG (2020) Standing dead trees contribute significantly to carbon budgets in Australian savannas. *International Journal of Wildland Fire*, WF19092.

Cuff N, Brocklehurst P (2015) Leaf and coarse fuel accumulation and relationships with vegetation attributes in 'evergreen' tropical eucalypt savannas. In 'Carbon accounting and savanna fire management'. (Eds B., Murphy, A., Edwards, M., Meyer, C., Meyer, J., Russell-Smith) pp. 169–181. (CSIRO Publications: Melbourne, Vic., Australia).

Eamus D, Chen X, Kelley G, Hutley LB (2002) Root biomass and root fractal analyses of an open Eucalyptus forest in a savanna of north Australia. *Australian Journal of Botany* **50**, 31-41.

Edwards AC, Russell-Smith J, Maier SW (2018). A comparison and validation of satellite-derived fire severity mapping techniques in fire prone north Australian savannas: Extreme fires and tree stem mortality. *Remote sensing of Environment* **206**, 287-299.

Fensham RJ, Bowmann DMJS (1992) Stand structure and the influence of overwood on regeneration in tropical eucalypt forest on Melville Island. *Australian Journal of Botany* **40**, 335–352.

Fensham RJ (2005) Monitoring standing dead wood for carbon accounting in tropical savanna. *Australian Journal of Botany* 53, 631-638.

Fensham RJ, Fairfax RJ (2007) Drought-related tree death of savanna eucalypts: Species susceptibility, soil conditions and root architecture. *Journal of Vegetation Science* **18**, 71-80.

Fensham, RJ, Fairfax RJ, Ward DP (2009) Drought-induced tree death in savanna. *Global Change Biology* **15**, 380-387.

Fensham RJ, Holman JE (1999) Temporal and Spatial patterns in drought related tree dieback in Australian savanna. *Journal of Applied Ecology* **36**, 1035-1050.

Fensham RJ, Freeman ME, Laffineaur B, Macdermott H, Prior LD, Werner PA (2017) Variable rainfall has a greater effect than fire on the demography of the dominant tree in a semi-arid *Eucalyptus* savanna. *Austral Ecology* **42**, 772-782.

Freeman M, Vesk PA, Murphy BP, Cook GD, Richards AE, Williams RJ (2017) Defining the fire trap: Extension of the persistence equilibrium model in mesic savannas. *Austral Ecology* **42**, 890-899.

Finlayson CM (1988) Productivity and nutrient dynamics of seasonally inundated floodplains in the Northern Territory. In: D. Wade Marshall and P. Loveday (Editors), Northern Australia: Progress and Prospects, Vol. 2.

Floodplains Research. ANU Press, Canberra, pp.58-83

Finlayson CM, Cowie ID, Bailey BJ (1993) Biomass and litter dynamics in a Melaleuca forest on a seasonally inundated floodplain in tropical, northern Australia. *Wetlands Ecology and Management* **4**, 177-188.

Guerschman JP, Hill MJ, Renzullo LJ, Barrett DJ, Marks AS, Botha, EJ (2009) Estimating fractional cover of photosynthetic vegetation, non-photosynthetic vegetation and bare soil in the Australian tropical savanna region upscaling the EO-1 Hyperion and MODIS sensors. *Remote Sensing of Environment* **113**, 928–945.

Grace J, Jose JS, Meir P, Miranda HS, Montes, RA (2006) Productivity and carbon fluxes of tropical savannas. *Journal of Biogeography* **33**, 387-400.

Hutley LB, Evans BJ, Beringer J, Cook GD, Maier SW, Raxon E (2013) Impacts of an extreme cyclone event on landscape-scale savanna fire, productivity and greenhouse gas emissions. *Environmental Research Letters* **8**.

Lawes MJ, Adie H, Russell-Smith J, Murphy B, Midgley JJ (2011) How do small savanna trees avoid stem mortality by fire? The roles of stem diameter, height and bark thickness. *Ecosphere*, **42**.

Lehmann, CER, Anderson TM, Sankaran, M *et al.* (2014) A Savanna vegetation-fire-climate relationships differ among continents. *Science* **343**, 548-552.

Levick SR, Richards AE, Cook GD, Schatz K, Guderle M, Williams RJ, Subedi, P, Trumbore SE, Anderson AN (2019). Rapid response of habitat structure and above-ground carbon storage to altered fire regimes in tropical savanna. *Biogeosciences* **16**, 1493-1503.

Liedloff AC, Cook GD (2007) Modelling the effects of rainfall variability and fire on tree populations in an Australian tropical savanna with the Flames simulation model. *Ecological Modelling* **201**, 269-282.

Liedloff AC, Cook GD (2011) The interaction of fire and rainfall variability on tree structure and carbon fluxes in savannas: Application of the Flames model. In: Ecosystem Function in Savannas: Measurement and Modeling at Land-scape to Global Scales. Eds, M. J. Hill , N. P. Hanan. pp. 293–308. CRC/Taylor and Francis, Boca Raton.

Lonsdale WM, Braitehwaite RW (1991) Assessing the effects of fire on vegetation in tropical savannas. *Australian Journal of Ecology* **16**, 363-374.

Lynch D, Russell-Smith J, Edwards AC, Evans J, Yates C (2018) Incentivising fire management in Pindan (Acacia shrublands): A proposed fuel type for Australia's savanna burning greenhouse gas emissions abatement methodology. *Ecological Management and Restoration* **19**, 230-238.

Maier SW, Russell_Smith J (2012) Measuring and monitoring of contemporary fire regimes in Australia using satellite remote sensing. In: Flammable Australia: Fire Regimes, Biodiversity and Ecosystems in a Changing Word.

(Eds R.A., Bradstock, A.M., Gill, R.J., Williams) pp. 293-306. CSIRO Publishing, Melbourne.

McIvor JG (2001) Litterfall from trees in semiarid woodlands of north-east Queensland. *Austral Ecology* **26**, 150-155.

Meyer CP, Cook G, Powell J (2015) Australia's national greenhouse gas inventory 2013: Agriculture. CSIRO Oceans and Atmosphere Flagship, Aspendale, Australia. 66p.

Meyer CP, Cook GD (2015) Biomass combustion and emission processes in the northern Australian savannas. "Carbon Accounting and Savanna Fire Management", Eds: Brett P. Murphy, Andrew C. Edwards, Mick Meyer and Jeremy Russell-Smith, CSIRO Publishing, Clayton Sth, Victoria, Australia, pp 185-205.

Murphy BP, Russell-Smith J, Prior LD (2010) Frequent fires reduce tree growth in northern Australian savannas: implications for tree demography and carbon sequestration. *Global Change Biology* **16**, 331-343.

Murphy BP, Liedloff AC, Cook GD (2015) Fire or water: which limits tree biomass in Australian savannas? "Carbon Accounting and Savanna Fire Management", Eds: Brett P. Murphy, Andrew C. Edwards, Mick Meyer and Jeremy Russell-Smith, CSIRO Publishing, Clayton Sth, Victoria, Australia, 2015, pp 273-294.

Murphy BP, Whitehead PJ, Evans J, Yates CP, Edwards AC, MacDermott HJ, Lynch DC, Russell-Smith, J (2022) Using a demographic model to project the long-term effects of fire management on tree biomass in Australian savannas. *Ecological Monographs* **e1564**

O'Grady APO, Chen X, Eamus D, Hutley LB (2000) Composition, leaf area index and standing biomass of eucalypt open forests near Darwin in the Northern Territory, Australia. *Australian Journal of Botany* **48**, 629-638.

Pasut C, Paul KI, Piper M, England JR, Roxburgh SH (2023) A new approach to monitor woody biomass change from canopy cover in rangeland ecosystems. *Journal of Applied Ecology*, In Review.

Paul KI, Larmour J, Specht A, Zerihun A, Ritson P, Roxburgh S, Sochachi S, Lewis T, Barton C, England JR, Battaglia M, O'Grady A, Pinkard E, Applegate G, Jonson J, Brooksbank K, Sudmeyer R, Wildy D, Montagu KD, Bardford M, Butler D, Hobbs T (2016) Testing the generality of below-ground biomass allometry across plant functional types at the continent scale. *Global Change Biology* **22**, 2106-2124.

Paul KI, Roxburgh SH, Larmour JS (2017) Moisture content correction: Implications of measurement errors on tree- and site-based estimates of biomass. *Forest Ecology and Management* **392**, 164-175.

Paul KI, Larmour JS, Specht A, Zerihun A, Ritson P, Roxburgh SH, Sochacki S, Lewis T, Barton C, England JR, Battaglia M, O'Grady A, Pinkard E, Applegate G, Jonson J, Brooksbank K, Sudmeyer R, Wildy D, Montagu KD, Bradford M, Butler D, Hobbs T (2019) Testing the generality of below-ground biomass allometry across plant functional types. *Forest Ecology and Management* **432**, 102-114.

Prior LD, Murphy BP, Russell-Smith J (2009) Environmental and demographic correlates of tree recruitment and mortality in north Australian savannas. *Forest Ecology and Management* **257**, 66-74.

Roxburgh SH, Karunaratne SB., Paul KI, Lucas RM, Armston JD, Sun J (2019) A revised above-ground maximum biomass layer for the Australian continent. *Forest Ecology and Management* **432**, 264-75.

Russell-Smith J, Murphy BP, Meyer CP, Cook GD, Maier S, Edwards AC, Brocklehurst P (2009) Improving estimates of savanna burning emissions for greenhouse accounting in northern Australia: limitations, challenges, applications. *International Journal of Wildland Fire* **18**, 1-18.

Thackway R, Auricht C, Edwards A, Lynch D, Cuff N (2014) A vegetation fuel type map for Australia's northern Savannas. Report prepared for the Department of the Environment, Canberra.

Werner PA, Murphy PG (2001) Size-specific biomass allocation and water content of above- and belowground components of three Eucalyptus species in a northern Australian savanna. *Australian Journal of Botany* **49**, 155-167.

Whitehead PJ, Murphy BP, Evans J, Lynch DC, Yates CP, Edwards AC, MacDermott HJ, Russell-Smith J (2022) Fire affects input and loss of dead wood. *Ecological Applications*. *In review*.

Wilson BA, Bowman DMJS (1987) Fire, storm, flood and drought: the vegetation ecology of Howards Peninsula, Northern Territory, Australia. *Australian Journal of Ecology* **12**, 165-174.

Williams RJ, Cook GD, Gill AM, Moore PHR (1999) Fire regime, fire intensity and tree survival in a tropical savanna in Northern Australia. *Australian Journal of Ecology* **24**, 50–59.

Williams, RJ, Zerihum A, Monntague KD, Hoffamn M, Hutley LB, Chen X (2005) Allometry for estimating aboveground tree biomass in tropical and subtropical eucalypt woodlands: towards general predictive equations. *Australian Journal of Botany* **53**, 607-619.

Yates CP., Russell-Smith J., Murphy BP, Desailly M, Evans J, Legge S, Lewis F, Lynch D, Edwards AC (2015) Fuel accumulation, consumption and fire patchiness in the lower rainfall savanna region in "Carbon Accounting and Savanna Fire Management", Eds: Brett P. Murphy, Andrew C. Edwards, Mick Meyer and Jeremy Russell-Smith, CSIRO Publishing, Clayton Sth, Victoria, Australia, 2015, pp 115 – 132.

Yates CP, MacDermott H, Evans J, Murphy BP, Russell-Smith J (2020) Seasonal fine fuel and coarse woody debris dynamics in north Australian savannas. *International Journal of Wildland Fire* **29**, 1109-1119.